https://doi.org/10.5194/egusphere-2024-813
Preprint. Discussion started: 4 April 2024

Propagation from Meteorological Drought to Hydrological Drought Using SPI and SPEI Combined with the Adapted Threshold Level Method

Giovana Cristina Santos de Medeiros[1], Samiria Maria Oliveira da Silva[1]

[1]Graduate Program in Hydraulic and Environmental Engineering – Water Resources, Department of Civil Engineering, Federal University of Ceará, Fortaleza-CE, 60400900, Brazil

Correspondence to: Giovana Cristina Santos de Medeiros (giovanacsm@alu.ufc.br)

Abstract. The hydrological response within a region is often nonlinear, influenced by various factors such as physiographic features, anthropogenic activities, and climate change. Considering the inherent complexity, our study focuses on investigating the propagation from meteorological drought to hydrological drought in the Banabuiú, Castanhão, and Orós reservoirs, located in the State of Ceará, Brazil. To achieve this, we used the Standardized Precipitation Index (SPI) to identify meteorological drought events, which uses precipitation data, alongside the Standardized Precipitation Evapotranspiration Index (SPEI), incorporating potential evapotranspiration in its calculations. For assessing hydrological drought, we used the Adapted Threshold Level Method (ATLM), which calculates the water balance between the supply (represented available reservoir volume) and the demand (including withdrawals for various uses and evaporation losses from the watershed). For all three reservoirs, drought events were characterized by their frequency, duration, severity, magnitude, and drought recovery time across three aggregated time scales of 12, 24, and 36 months. To determine the propagation time from meteorological to hydrological drought, we calculated three indicators, corresponding to time differences between the onsets, peaks, and conclusions of the propagated drought events. Results indicated no significant differences in meteorological drought characteristics between SPI and SPEI methods. However, the SPEI showed higher values for meteorological drought in the Orós watershed. Analysis of drought propagation, employing different methods, revealed no defined pattern for the onset, peak, and end intervals across all tested combinations. Hence, we recommended utilizing all three indicators to enable a more comprehensive analysis of drought events propagated within the watersheds.

1 Introduction

Population growth and the expansion of the agricultural, energy, and industrial sectors have led to increased water demand to meet human and production needs (Wang et al., 2020). Conversely, there has been a reduction in water supply due to more frequent and pronounced extreme weather events (Mohor and Mendiondo, 2017).

Drought periods occur when water availability falls below normal levels, failing to meet human or environmental needs (Wilhite and Pulwarty, 2018). Typically, drought develops slowly and can have severe impacts on water resources, the

https://doi.org/10.5194/egusphere-2024-813
Preprint. Discussion started: 4 April 2024

environment, human life, and socio-economic activities (Choat et al., 2018). Therefore, improving drought characterization is crucial for enhancing monitoring, management, and forecasting efforts (Bevacqua et al., 2021).

Droughts are typically classified into four types based on the different types of water deficit: meteorological drought, hydrological drought, agricultural drought, and socioeconomic drought (Mishra and Singh, 2010; Wilhite and Glantz, 1985). These types of drought are closely interconnected because water stocks in the atmosphere, surface, and subsoil are interconnected within the hydrological cycle (Zhang et al., 2022a).

Research has indicated that meteorological drought, with its earlier onset, is widely recognized as the origin to other types of drought (Chen et al., 2020; Wu et al., 2017). Prolonged below-average precipitation impairs soil moisture retention and lowers water flows in bodies of water, intensifying agricultural and hydrological droughts, respectively (Zhang et al., 2022a). The transition from one type of drought to another is termed drought propagation (Eltahir and Yeh, 1999), a subject extensively studied to improve water resource management (Guo et al., 2020; Ma et al., 2019).

Given that prolonged precipitation deficits can propagate through various terrestrial phases of the hydrological cycle, understanding how the atmospheric signal modulates as it traverses through soils, watercourses, and aquifers is crucial for forecasting and developing effective drought mitigation policies (Raposo et al., 2023). In addition, this understanding serves as an early warning tool for this phenomenon (Wu et al., 2021a).

Although several studies have focused on explaining the propagation of meteorological drought to hydrological drought (Bevacqua et al., 2021; Guo et al., 2020; Huang et al., 2017; Wu et al., 2021a; Xu et al., 2019; Zhang et al., 2023), there remain some gaps requiring to be addressed. Sadhwani and Eldho (2024), for instance, investigated the characteristics and propagation time of meteorological-to-hydrological drought across different time scales using standardized indices, while considering future climate change scenarios. They concluded that identifying hydrological drought is more complex than meteorological drought due to the influence of diverse human activities, such as irrigation, industrial supply, urbanization, and watershed characteristics. This underscores the need for further research to quantify the effects of these factors on hydrological drought and its propagation.

Another factor contributing to the complexity of drought propagation involves the existing methods utilized. Among these, the maximum correlation method (Ho et al., 2021; Xing et al., 2021; Ding et al., 2021; Wu et al., 2021b; Zhou et al., 2021) and the theory of runs (Bevacqua et al., 2021; Chen et al., 2020; Ma et al., 2019; Guo et al., 2020) stand out as the most commonly used. In the maximum correlation method, propagation time is typically determined through correlation analysis between the time series of standardized drought indices, applicable across multiple time scales. However, since the entire time series is considered, encompassing both dry and wet periods, the emphasis is placed on the relationship between precipitation and flow rather than the propagation of drought (Raposo et al., 2023). On the other hand, the theory of runs often involves setting a certain threshold level. When each type of drought falls below this threshold, that moment is considered the beginning of the event for that type of drought. The difference between the onset times of the two drought events types is considered as the propagation time (Wu and Chen, 2019). However, this method assumes drought propagation to be a linear process, which may not hold true in many situations (Wu et al., 2017).

https://doi.org/10.5194/egusphere-2024-813
Preprint. Discussion started: 4 April 2024

Bevacqua et al. (2021) observed that analyzing the correlation between drought indices alone does not fully capture the dynamics of drought propagation. Additionally, they noted significant variations in the timing of drought onset, peak, and conclusion across different cases. In light of these findings, they suggest adopting multi-indicator approaches to identify the mechanisms of drought development and propagation throughout the hydrological cycle.

The literature indicates that drought propagation is primarily associated with the climatic, physical, and land use characteristics of the watershed (Huang et al., 2015; van Loon and Laaha, 2015). In this context, the use of methodologies for identifying hydrological droughts that incorporate data on watershed land use and occupation, as well as on water demand from sectors most commonly affected by drought, fills the existing gap in analyzing the propagation from meteorological drought to hydrological drought. Instead of relying solely on standardized hydrological drought indices, which primarily focus on changes in reservoir inflow, employing the Threshold Level Method (TLM) enables for quantification of the actual water deficit in the watershed using real series data rather than normalized variables (van Huijgevoort et al., 2012; van Loon and Laaha, 2015). This method offers a more effective approach to managing water resources at a local level (van Loon, 2015).

Therefore, this study aims to investigate the propagation from meteorological drought to hydrological drought in the Banabuiú, Castanhão, and Orós reservoirs located in the State of Ceará, Brazil. In this region, multi-year droughts are prevalent, including the recent six-year drought (2012-2018), which significantly impacted on water storage, agriculture, livestock, and industry (Marengo et al., 2018; Pontes Filho et al., 2020).

In order to identify meteorological drought events, we employed the Standardized Precipitation Index (SPI) and the Standardized Precipitation Evapotranspiration Index (SPEI). For assessing hydrological drought, we utilized the Adapted Threshold Level Method (ATLM). Drought events were characterized by their frequency, duration, severity, magnitude, and recovery across different time scales, with data aggregated for 12, 24, and 36 months. To determine the propagation time from meteorological drought to hydrological drought, we calculated three indicators corresponding to the time differences between the onsets, peaks, and ends of the propagated drought events.

2 Materials and Methods

2.1 Area of Study

The study area includes the Jaguaribe and Banabuiú Valleys, located within the Jaguaribe watershed in the state of Ceará, Brazil. This watershed spans a total area of 74,000 km², representing approximately 50% of the state's territory. It comprises of five sub-watersheds: the Upper, Middle, and Lower Jaguaribe, Banabuiú, and Salgado. Ceará predominantly features a semi-arid climate, with around 95.1% of its area of its area classified as such. The region is monitored by 153 reservoirs are monitored, of which 39 completely collapsed and another 42 fell below the minimum operational water level during the recent multi-year drought between 2012 and 2018 (Oliveira et al., 2022).

Consequently, the watersheds of the three main monitored reservoirs in this region were selected: Banabuiú (with an accumulation capacity of 1,534.00 hm³), Castanhão (with an accumulation capacity of 6,700.00 hm³), and Orós (with an

https://doi.org/10.5194/egusphere-2024-813
Preprint. Discussion started: 4 April 2024

accumulation capacity of 1,940.00 hm³). These reservoirs are located in the Banabuiú, Middle Jaguaribe, and Upper Jaguaribe sub-watersheds, respectively.

The Banabuiú and Castanhão dams are located downstream within the watershed, running parallel to each other, while the Orós Dam is situated at the exutory of the Upper Jaguaribe sub-watershed. The Orós Dam plays a crucial as a water source for the Middle and Lower Jaguaribe regions, ensuring the continuous flow of the Jaguaribe River until it reaches the Castanhão dam (see Figure 1) (SRH, 2011).

These reservoirs were selected due to their strategic significance to the state of Ceará, as they supply water for various purposes including drinking, agriculture, livestock, and other economic activities across multiple municipalities in the state (Gonçalves et al., 2023).

The climate in this region is characterized as hot, tropical, and semi-arid, with average annual temperatures ranging from 26 to 28°C and an average rainfall of approximately 700 mm. High evaporation rates, coupled with spatial and temporal variability of precipitation – a hydroclimatic trait of Ceará – result in a significant water deficit, leading to the formation of intermittent rivers. These rivers typically flow during the state's rainy season, occurring from January to April (Batista et al., 2019).

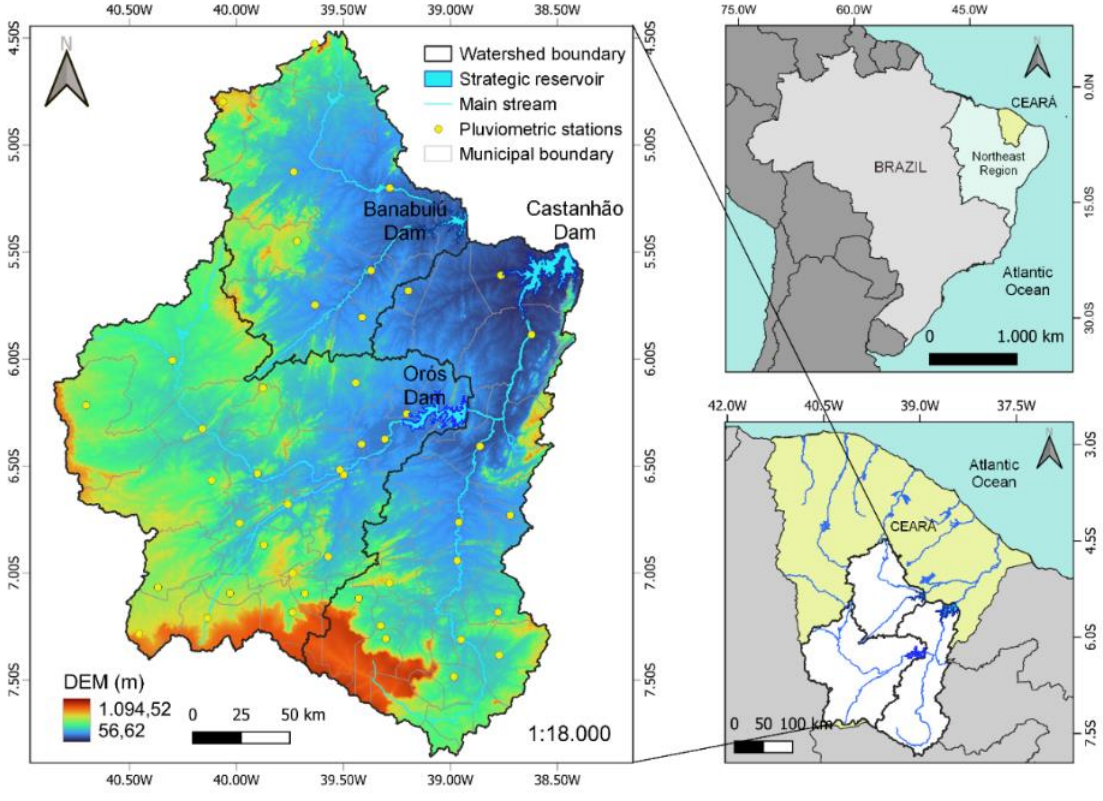

Figure 1. Location of the watershed of the Banabuiú, Castanhão and Orós, reservoirs in the State of Ceará, Brazil.

https://doi.org/10.5194/egusphere-2024-813
Preprint. Discussion started: 4 April 2024

2.2 Data Collection

The monthly precipitation data for the watershed of the studied reservoirs were sourced from FUNCEME, spanning from 1974 to 2023. Rain gauge stations with more than 30 years of data were selected and then interpolated using the Inverse Distance Weighting (IDW) method to derive the regional average monthly precipitation for each reservoir watershed.

Evaporation data covering the period from 1980 to 2010 were obtained from the climatological normals. These data corresponded to the nearest stations with available data: Jaguaruana Station (Code 82493) for the Castanhão Dam, Iguatu Station (Code 82686) for the Orós Dam, and Quixeramobim Station (Code 82586) for the Banabuiú Dam. These datasets were retrieved from the National Institute of Meteorology (INMET) website.

Monthly potential evapotranspiration data spanning from 1901 to 2020 were obtained from the Climatic Research Unit (CRU). The original data has a spatial grid resolution of 0.5° latitude by 0.5° longitude and it covers all global land areas. For our study region, we used specific spatial and temporal delineations. Spatial delineations were tailored to each reservoir under analysis, while temporal delineations were based on the availability of precipitation data for the same period (1974 – 2020).

The historical reservoir monitoring data for the Banabuiú and Orós dams were provided by FUNCEME, covering the period from 1986 and 2023. For the Castanhão dam, the data was made available from the start of its operation in 2004 until 2023. The stored volumes were computed by monitoring the reservoir levels and using the Quota-Area-Volume (QAV) ratio of each reservoir to estimate the monthly volume based on the water level. Similarly, the evaporated volumes were estimated by multiplying the monthly evaporation rates, obtained from the climatological normals, by the surface area of the lake on the first day of each month.

Data on the demands for each reservoir were obtained from the Seminar on Negotiated Allocation of the Waters of the Jaguaribe and Banabuiú Valleys, organized by the Water Resources Management Company (COGERH) in July 2023. This seminar determines the flows to be released for various purposes based on allocation scenarios, using the year 2022 as a reference.

2.3 Methodology

In this study, we utilized the widely recognized Standardized Precipitation Index (SPI), developed by McKee et al. (1993), and the Standard Precipitation Evapotranspiration Index (SPEI, proposed by Vicente-Serrano et al. (2010)), to determine meteorological drought. For evaluating hydrological drought, we used the Adapted Threshold Level Method (ATLM), as developed by Medeiros et al. (2019).

Across all three cases, drought events were characterized by their frequency, duration, severity, magnitude, and recovery time, with data aggregated for 12, 24, and 36 months. However, due to the inherent limitations in the methodologies used, our analysis focused on comparing the periods of identified drought events to understand the occurrence of drought propagation in the study region.

https://doi.org/10.5194/egusphere-2024-813
Preprint. Discussion started: 4 April 2024

2.3.1 Standardized Precipitation Index (SPI)

To analyze the meteorological drought events spanning from 1974 and 2023 in the Castanhão, Orós, and Banabuiú reservoirs, we employed the Standardized Precipitation Index (SPI). Developed by McKee, Doesken, and Kleist (1993), SPI is derived by fitting precipitation data to the gamma probability distribution. Subsequently, the probabilities of occurrence for each precipitation value are calculated by applying the inverse of the normal distribution, thereby identifying deviations from the average precipitation for the analyzed intervals (Angelidis et al., 2012; Zhang et al., 2017). A drought event commences whenever the index value turns negative and persists until it rises above zero again (McKee et al., 1993).

SPI is used widely worldwide due to its versatility in analyzing both drought and flood periods, ease of calculation, and requirement of only precipitation data. However, it is recommended to use SPI with a series of monthly values spanning at least 30 years, ideally extending to 50 and 60 years (WMO, 2012).

For our analysis, we used SPI-12, SPI-24, and SPI-36, representing twelve, twenty-four, and thirty-six months respectively. These periods allow for examining the effects of drought across different sectors and on water scarcity (Araújo Júnior et al., 2020). Additionally, longer time scales of SPI tend to exhibit stronger correlation with hydrological drought indicators (Keyantash, 2023).

2.3.2 Standardized Precipitation Evapotranspiration Index (SPEI)

The Standardized Precipitation Evapotranspiration Index (SPEI) was proposed by Vicente-Serrano et al. (2010) and is calculated by determining the difference (D) between precipitation (PRC) and evapotranspiration (PET) for each month (t), as described in Eq. (1).

$$D_t = PRC_t - PET_t, \quad (1)$$

SPEI follows the same procedure as SPI and involves converting the log-logistic distribution into the standard normal distribution. Similar to SPI, SPEI is calculated using aggregated data for 12, 24, and 36 months (SPEI-12, SPEI-24, and SPEI-36). Further, details of the methodology can be found in the study of Vicente-Serrano et al. (2010).

2.3.3 Adapted Threshold Level Method (ATLM)

The Threshold Level Method serves as a valuable tool for quantifying hydrological drought by assessing the water volume below a specific threshold, thereby allowing for the determination of drought characteristics such as duration, severity, and magnitude. In this study, we adapted the threshold level method originally developed by Medeiros et al. (2019), which defines hydrological drought as occurring when the reservoir's storage volume falls below a predetermined threshold.

This threshold level accounts not only water losses due to evaporation but also losses stemming from the demands of various uses. Additionally, our study incorporated time factors (tf) of 12, 24, and 36 months, representing future periods during which the accumulated water in the reservoir at time *t* can meet the demands while also accounting for evaporation losses.

https://doi.org/10.5194/egusphere-2024-813
Preprint. Discussion started: 4 April 2024

These time periods were selected to align with the analysis of drought propagation using the SPI and SPEI meteorological drought indices.

Using the same time factor (tf), the threshold level (TL(tf)) was determined by summing the withdrawals needed to fulfill all the demands associated with the reservoir (Dem(tf)) and the evaporated volume (EVP(tf)), as shown in Eq. (2).

$$TL(tf) = Dem(tf) + EVP(tf), \quad (2)$$

The value of EVP(tf) was calculated using Eq. (3), where *t* represents the time in months, *E* is the historical average of the lake's monthly evaporation in meters per month (m.month^{-1}), *PRC* is the historical average of the monthly precipitation in meters per month (m.month^{-1}), and *A* is the area in square meters (m²) on the first day of each month of the reservoir watershed monitoring data series:

$$EVP(tf) = \sum_{t=1}^{tf}\{ [E(t) - PRC(t)] * A(t)\}, \quad (3)$$

The hydrological variable used for calculating the water deficit is the monthly reservoir storage volume (Vol(t)), obtained from the monitoring records maintained by FUNCEME-CE. Thus, the volume of water deficit (WD(tf)) was computed using Eq. (4).

$$WD(tf) = Vol(t) - TL(tf), \quad (4)$$

In the event of WD(tf) < 0, a hydrological drought occurs, which persists until the volume stored in the reservoir exceeds the threshold level considered in the analysis (WD(tf) >= 0).

2.3.3 Characterization of droughts

Characterization of droughts was conducted for each reservoir and each index, encompassing the determination of the number of drought events, their frequency, duration, severity, intensity or magnitude, and recovery time following a drought event (both meteorological and hydrological).

Frequency was calculated by dividing the total number of months experiencing drought by the total number of months analyzed. Duration represents the time, in months, from the onset (t_{begin}) to the conclusion (t_{end}) of each drought event. The severity of meteorological drought was determined by summing the SPI and the SPEI values, for each index respectively, while the severity of hydrological drought was evaluated based on the sum of the Water Deficit values. Intensity or magnitude of the drought was determined by dividing its severity by its duration. Furthermore, drought recovery time (r_{time}) was determined by establishing the duration it takes for a drought event to subside after reaching its peak severity. Thus, drought recovery time was calculated by subtracting the end month (t_{end}) from the peak month (t_{peak}) of the event.

https://doi.org/10.5194/egusphere-2024-813
Preprint. Discussion started: 4 April 2024

2.3.4 Mutually dependent droughts and minor droughts

In this study, the definition of meteorological and hydrological wet and dry periods adheres to the theory of runs, as introduced by Yevjevich (1967). According to this theory, a series of drought events below a certain threshold level may include periods intermittent, low-magnitude wet event occurring between two consecutive drought events. In such cases, droughts are considered mutually dependent, necessitating their grouping to establish a consistent definition of drought events (Tallaksen et al., 1997). To achieve this grouping, we employed the Inter-Event Time Method (IT Method), introduced by Zelenhasic and Salvai (1987), as depicted in Figure 2.

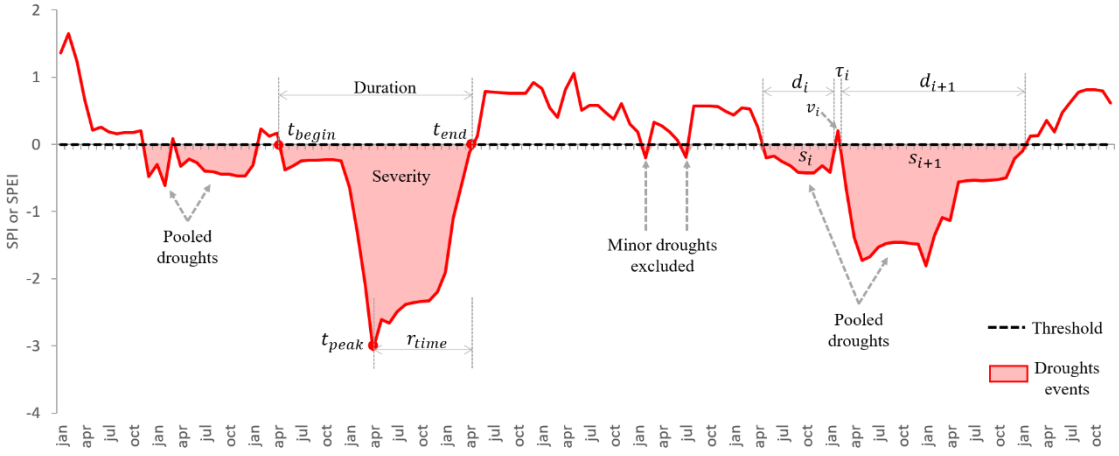

Figure 2. Representation of the characteristics of drought events, including duration, severity, and drought recovery time ($\mathbf{r_{time}}$), based on the scale of the SPI and SPEI meteorological drought indices. The same characterization was conducted for hydrological drought using the ATLM. For illustrative purposes, random data were used to demonstrate the pooling of mutually dependent droughts and the exclusion of minor droughts.

In this approach, two mutually dependent droughts are consolidated if the duration between them is less than a predefined number of days (tc), specifically if $\tau i \leq tc$. The duration of a pooled drought event ($DDpooled$) is therefore defined from the first day of the first drought event to the last day of the cluster's last drought event, including the excess period (τi) (Eq. 5). For this study, a tc of one month was chosen.

$$DDpooled = d_i + d_{i+1} + \tau_i, \quad (5)$$

On the other hand, minor droughts are characterized by being short-lived and low deficit volume. A multitude of minor droughts can distort the analysis of drought frequency over time, necessitating the exclusion of minor droughts (Tallaksen et al., 1997). Accordingly, all drought events lasting one month or less were excluded from the analysis.

https://doi.org/10.5194/egusphere-2024-813
Preprint. Discussion started: 4 April 2024

Following the exclusion of minor droughts and the establishment of the duration of the pooled drought, the severity of the pooled drought ($DSpooled$) was determined by summing the deficit volumes and subtracting the excess volume of the intermediate event (Eq. 6).

$$DSpooled = s_i + s_{i+1} - v_i, \quad (6)$$

In studies addressing reservoir management, subtracting the excess volume from the total of the deficit volumes offers a more accurate depiction of reservoir withdrawal and replenishment processes (Fleig et al., 2006). This approach has been adopted by Chen et al. (2013), Pandey et al. (2008), Sung and Chung (2014) and Tallaksen et al. (1997).

2.3.5 Propagation of droughts

The determination of the propagation time from meteorological drought to hydrological drought was obtained through the calculation of three indicators, as outlined by Bevacqua et al. (2021). The first indicator concerns the time differences between the beginnings of each meteorological drought and hydrological drought event (Δb), the second corresponds to the time difference between the peaks of these events (Δp). The third indicator involves the time differences between the ends of the events (Δe) (Figure 3). To determine hydrological drought resulting from a meteorological drought, it was established that (i) the meteorological drought must begin before the hydrological drought, (ii) the hydrological drought must start before the meteorological drought ends, and (iii) the peak and end of the meteorological drought must occur before the peak and end of the hydrological drought.

The total propagation time can thus be determined by averaging the time intervals between the onset, peak, and end time intervals of drought events propagated in the study area (Zhang et al., 2022a; Wu et al., 2021b).

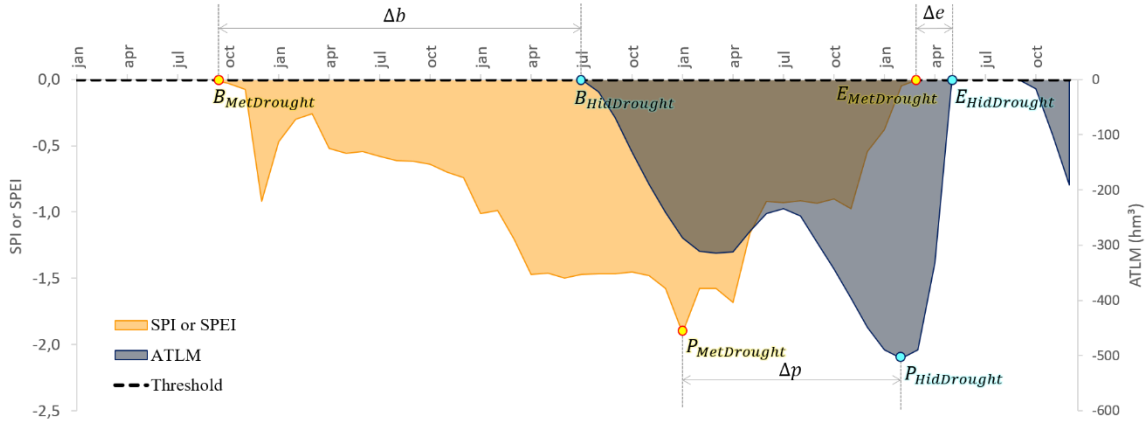

Figure 3. Propagation of the different types of drought using indicators that determine the time difference between the onsets (Δb), peaks (Δp), and ends (Δe) of the meteorological and hydrological droughts. Random data were used for illustrative purposes to demonstrate the calculation of the indicators under predefined conditions. $\boldsymbol{B_{MetDrought}}$ and $\boldsymbol{B_{HidDrought}}$ denote the beginning month, $\boldsymbol{P_{MetDrought}}$ and

https://doi.org/10.5194/egusphere-2024-813
Preprint. Discussion started: 4 April 2024

$P_{HidDrought}$ denote the peak month, and $E_{MetDrought}$ and $E_{HidDrought}$ denote the end month of the meteorological drought (SPI or SPEI) and hydrological drought (ATLM), respectively.

3 Results and Discussion

3.1 Characterization of Meteorological Drought Using the SPI and SPEI Indices

The values of the meteorological drought indices were determined for the annual (12 months), biennial (24 months), and triennial (36 months) time scales, spanning from 1975 to 2023 for the SPI and from 1975 to 2020 for the SPEI. In Figures 4, 5, and 6, only the periods in which the indices fell below 0.0 (defined as the drought threshold) are depicted for the watersheds of the Banabuiú, Castanhão, and Orós reservoirs, respectively.

In the case of the Banabuiú watershed, the meteorological droughts accumulated over 12 months (SPI-12 and SPEI-12) had the highest number of drought occurrences, with 16 events, occurring approximately 50% of the time (Figure 7). For long-term scales, a lower number of event occurrences was observed while maintaining the same frequency, indicating that once a drought occurs, it has a longer duration. This trend was similarly observed in the watershed of the Castanhão Dam.

However, for the Orós Reservoir watershed, the SPI index indicated a high frequency of meteorological drought events across time scales aggregated for 12, 24, and 36 months, resulting in drought conditions 60%, 61%, and 62% of the time, respectively. On the other hand, the SPEI index showcased a behavior similar to that of the other reservoirs, exhibiting an average frequency of around 50% and a decreasing number of events as the index scale increased (see Figure 7).

https://doi.org/10.5194/egusphere-2024-813
Preprint. Discussion started: 4 April 2024

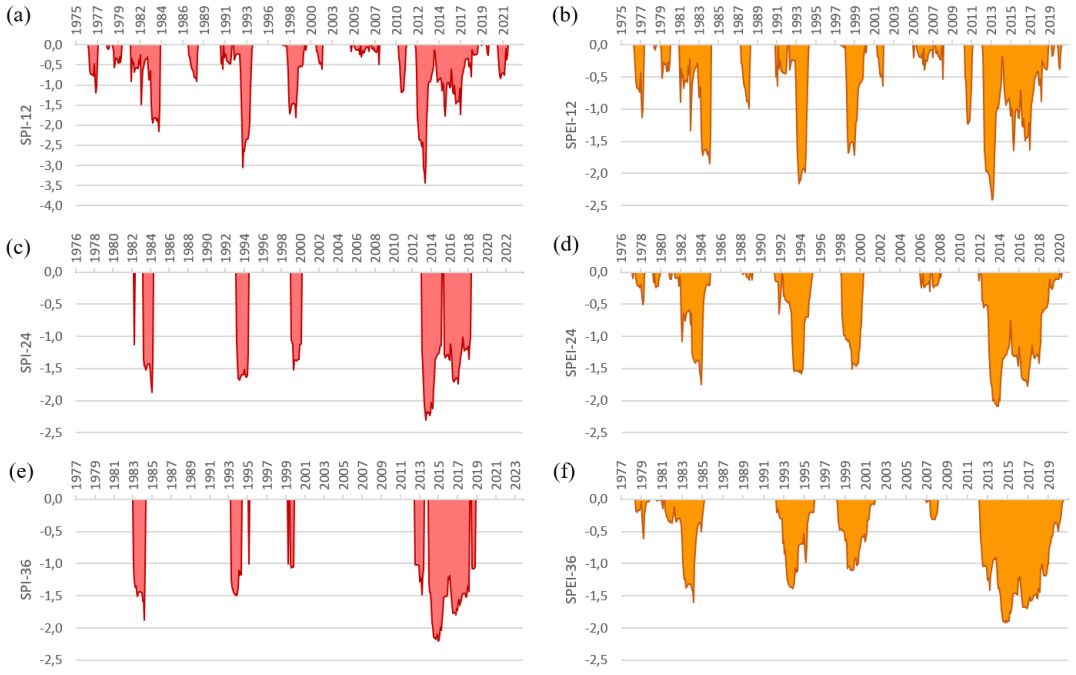

Figure 4. Periods of meteorological drought identified using the SPI and SPEI indices for the Banabuiú Dam, at time scales with data aggregated for 12, 24, and 36 months.

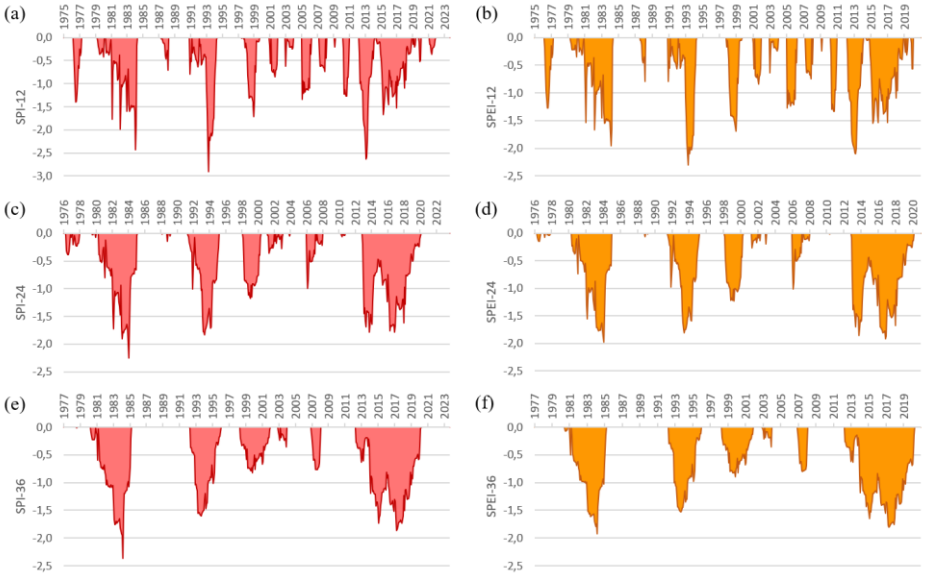

Figure 5. Periods of meteorological drought identified using the SPI and SPEI indices for the Castanhão Dam, at time scales with data aggregated for 12, 24, and 36 months.

https://doi.org/10.5194/egusphere-2024-813
Preprint. Discussion started: 4 April 2024

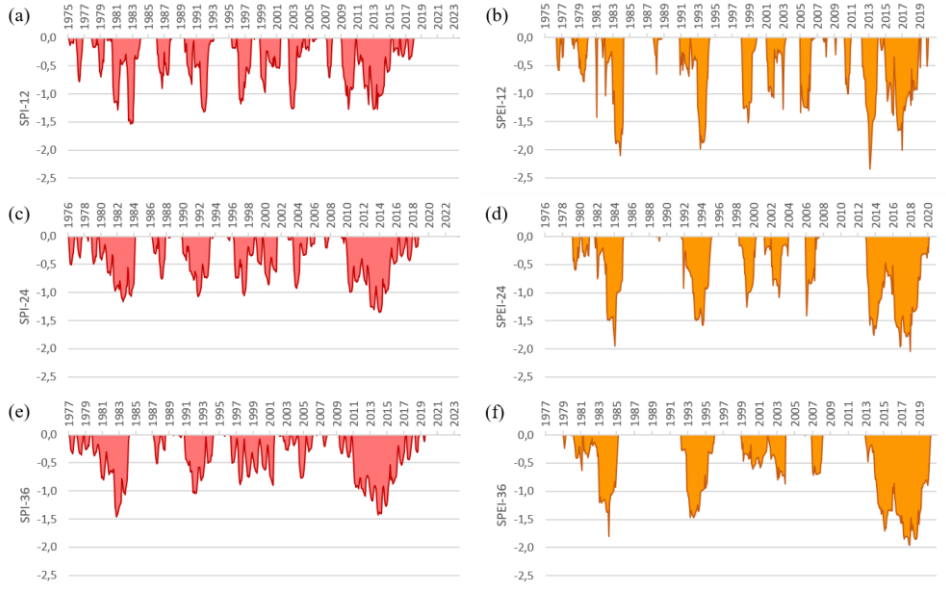

Figure 6. Periods of meteorological drought identified using the SPI and SPEI indices for the Orós Dam, at time scales with data aggregated for 12, 24, and 36 months.

Analyzing the average duration of drought events identified using the SPI and SPEI indices for the Banabuiú and Castanhão watersheds reveals no significant difference between the indices for the same time scale with aggregated data (Figure 8a). However, the durations of meteorological drought periods are notably longer at the time scale with data aggregated for 36 months compared to the other time scales. It is noteworthy that in the case of the Banabuiú watershed, the event with the longest duration started in March 2012 and lasted until the end of 2018, according to the SPI-12 (Figure 4a) and SPEI-12 (Figure 4b), persisting for 82 and 83 months, respectively. According to the SPI and SPEI over 24 and 36 months, this same drought event extended until the first half of 2020 (Figure 4c e Figure 4d).

In the Castanhão watershed, the longest meteorological drought, lasting 54 months, occurred during the same period, beginning two years after it began in the Banabuiú watershed, in June 2014, according to the SPI-12 and SPEI-12 indices (Figure 5a e Figure 5b). For time scales with data aggregated for 24 and 36 months, the prolonged extreme event detected by the indices occurred between 2012 and 2020, lasting up to 96 months (Figure 8a).

In the case of the Orós Dam watershed, the average duration of drought events was 21 and 19 months, according to the SPI-12 and SPEI-12 indices, respectively (Figure 8a). Considering the SPI and SPEI with data aggregated for 24 and 36 months, the SPEI-36 stands out for its wide variation in the minimum and maximum duration of drought events.

https://doi.org/10.5194/egusphere-2024-813
Preprint. Discussion started: 4 April 2024

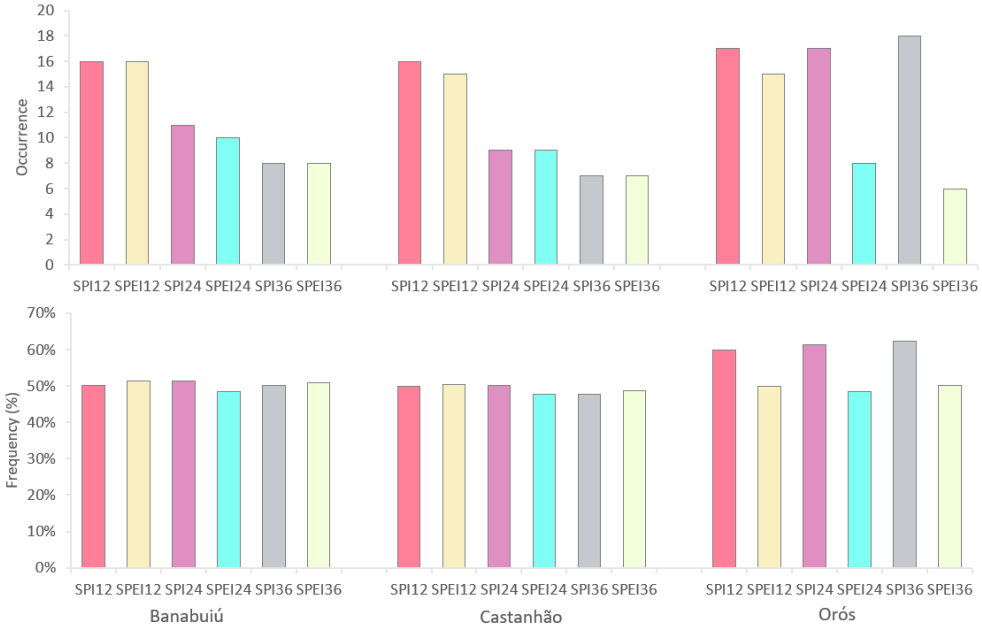

Figure 7. Number of occurrences and frequency of meteorological drought events for the watersheds of the Banabuiú, Castanhão, and Orós reservoirs.

The longest drought in this watershed began and ended earlier compared to the other watersheds studied, according to the SPI-12 (February 2009 to March 2015), SPI-24 (May 2009 to March 2016), and SPI-36 (May 2009 to March 2017) indices (Figure 6a, Figure 6c, and Figure 6e). The longer drought periods identified using the SPEI corresponded approximately to the same period as those in the Banabuiú and Castanhão watersheds (2012–2020).

Thus, the meteorological drought indices studied indicate that the multi-year drought that began in 2012 was the longest in the historical series analyzed, leading to negative effects in various sectors such as agriculture, livestock, and surface and underground resources. There has been a decline in water storage in the strategic reservoirs monitored by COGERH, resulting in a scarcity of water supply in cities, animal mortality, increased migration, and losses in agriculture (De Brito, 2021; Marengo et al., 2016; Rabelo and Lima Neto, 2018). According to Marengo et al. (2016), this event may be associated with unusual cloud formation patterns due to the position of the Intertropical Convergence Zone (ITCZ) and the presence of the La Niña phenomenon, which resulted in the opposite of what was expected—an increase in rainfall trends.

https://doi.org/10.5194/egusphere-2024-813
Preprint. Discussion started: 4 April 2024

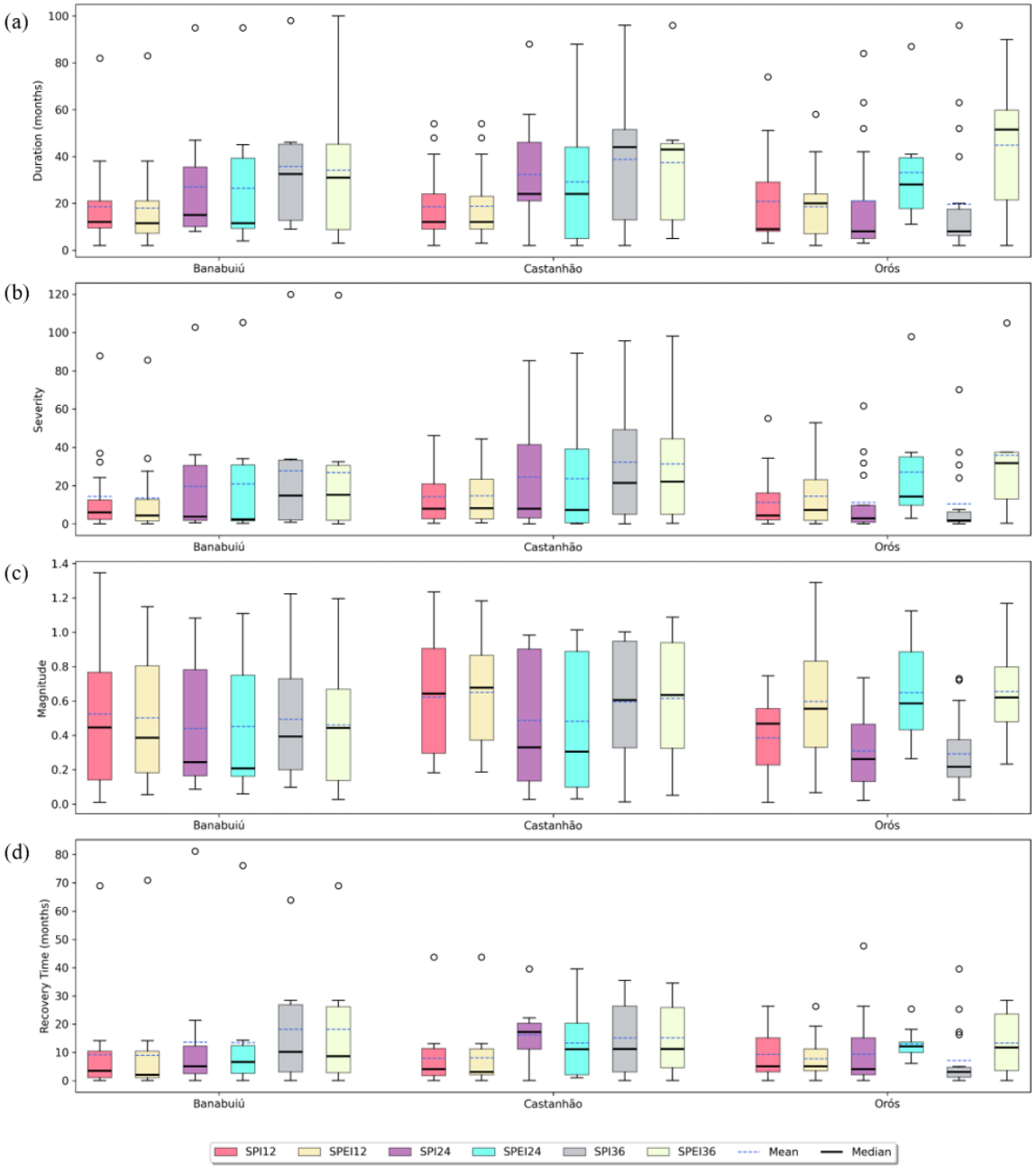

Figure 8. Characteristics of meteorological drought identified using the SPI and SPEI indices at the time scale with data aggregated for 12, 24, and 36 months for the watersheds of the Banabuiú, Castanhão, and Orós reservoirs: (a) duration (months); (b) severity (dimensionless); (c) magnitude (dimensionless); (d) recovery time from drought events (months). The hollow circles represent the values of extreme events.

300 These extended periods of drought also tend to exhibit the most severe impacts, as evidenced across all the analyses conducted on the indices and watersheds under study. In the Banabuiú watershed, for example, both the SPI-12 and SPEI-12 indices

https://doi.org/10.5194/egusphere-2024-813
Preprint. Discussion started: 4 April 2024

indicated events with severity peaking at high values of 87 and 85, respectively. Furthermore, when examining longer time frames with data aggregated for 24 and 36 months, the severity of drought events remained notably high, with the SPI-24 reaching 103 and the SPI-36 reaching 120 (Figure 8b). Similarly, in the Castanhão watershed, there was a certain similarity between the SPI and SPEI indices during the same periods (Figure 8b). Additionally, it is observed that the average severity increases with the addition of more months in the indices, as anticipated.

Considering the assessment of drought magnitude, which reflects the intensity of the events, the SPI and SPEI indices exhibit comparable patterns at equivalent time scales for the Banabuiú and Castanhão reservoirs (Figure 8c). For the Orós Reservoir watershed, in turn, the average drought intensity appears higher, particularly according to the SPEI index. This result may suggest that the influence of evapotranspiration on the SPEI calculation has a more pronounced impact on drought characteristics in the Orós watershed compared to Banabuiú and Castanhão.

When examining the recovery time from drought events, there appears to be no notable difference on average between the SPI and SPEI indices at the same aggregated time scale, especially evident in the Banabuiú and Castanhão watersheds (Figure 8d). Notably, extreme events where the peak severity of the longest-duration droughts initiates the recovery process can take up to 81 months to return to a normal state. An example of this is the drought that started in April 2012, reached its severity peak in May 2013, and ended in January 2020, as identified by the SPI-24 for the Banabuiú watershed.

Overall, there were no significant differences in the main characteristics of drought between the SPI and SPEI indices across the studied watersheds in the Banabuiú and Castanhão regions. For the Orós watershed, in turn, the SPEI tends to exhibit relatively higher values in drought characteristics compared to the SPI. While certain studies suggest that the SPEI might be more adept at characterizing meteorological drought (Li et al., 2020; Pei et al., 2020), it is important to consider that the most suitable index actually depends on various factors such as the region's topography, soil cover, and the purpose of drought monitoring (Gumus, 2023).

3.2 Characterization of Hydrological Drought Using the Adapted Threshold Level Method (ATLM)

The water deficits for the times factors of 12, 24, and 36 months of the Banabuiú, Castanhão, and Orós Dams are depicted in Figure 9. For a better understanding, only the negative values of the deficit are shown in the figure.

https://doi.org/10.5194/egusphere-2024-813
Preprint. Discussion started: 4 April 2024

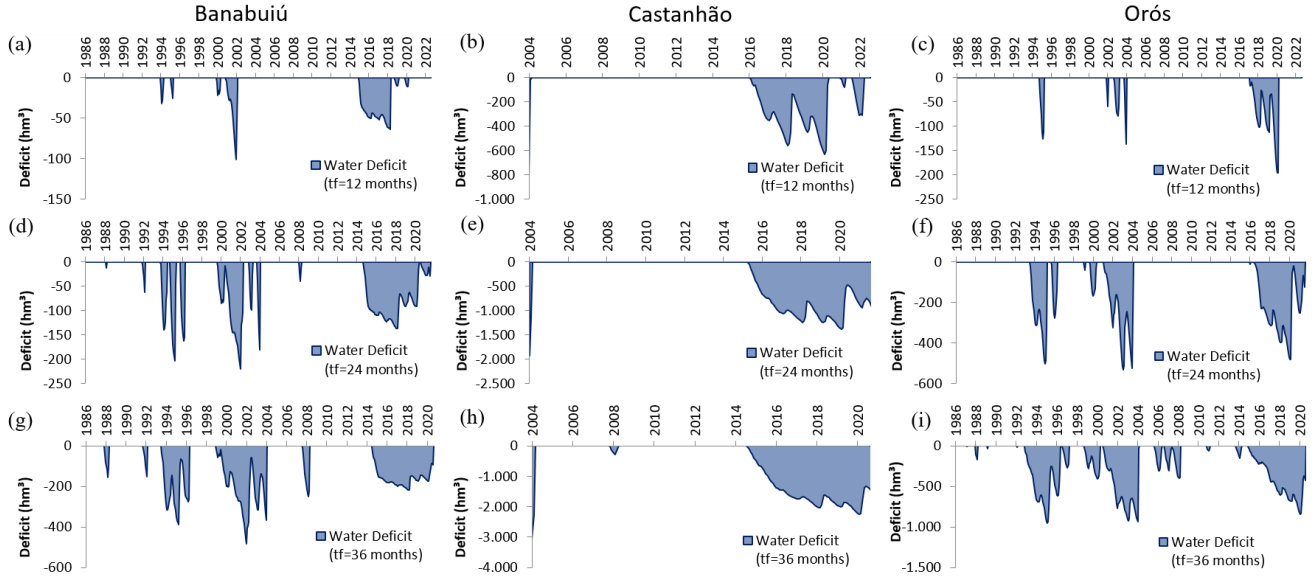

Figure 9. Drought periods identified for the Banabuiú, Castanhão, and Orós dams using the ATLM, considering time factors with data aggregated for 12, 24, and 36 months.

As the time factor increases, drought events tend to begin earlier, and the intervals between them shorten, ultimately leading to prolonged periods of hydrological drought across the historical series for the analyzed reservoirs, particularly noticeable in the Orós and Banabuiú Dams. Moreover, there is a notable escalation in the volume of water deficit over time. While this pattern is observed across all three reservoirs, it is most pronounced in the Orós and Banabuiú Dams. It's worth mentioning that historical data for the Castanhão Dam is limited due to its operation commencing only in 2004. Nevertheless, as the largest water reservoir in the State of Ceará, with a total capacity of 6,700 hm³, it was engineered to withstand more extreme drought conditions.

Analyzing the number of occurrences and frequency of hydrological drought events, it's revealed that the Banabuiú Dam experienced the highest number of events with a time factor of 24 months (9 events). For the Castanhão Dam it was with a time factor of 12 months (4 events), and for the Orós Dam with a time factor of 36 months (10 events) (Figure 10). This suggests that there is no direct proportional relationship between the increase in time factor and the occurrence of drought events across all studied reservoirs. However, concerning frequency, there is a clear proportionality – the higher the time factor used, the longer the reservoir experiences hydrological drought throughout the historical series. For instance, the frequency of drought at the Orós Dam increased from 12% to 55% for time factors of 12 and 36 months, respectively (Figure 10).

The periods of water deficit depicted in Figure 9 were further characterized by their duration, severity, magnitude, and drought recovery time, as shown in Figure 11.

The analysis of the Banabuiú Dam revealed that, with a time factor of 12 months, the longest-lasting event spanned 42 months, exhibiting the highest severity (1,861.87 hm³), consequently resulting in the greatest magnitude (44.79 $hm^3.month^{-1}$) among all identified events. Occurring from January 2015 to May 2018, the reservoir maintained an average capacity of merely

https://doi.org/10.5194/egusphere-2024-813
Preprint. Discussion started: 4 April 2024

1% of its maximum capacity, underscoring a significant and prolonged water deficit. On average, the droughts lasted 11 months, with typical severity and magnitude values of 397.90 hm³ and 22.08 hm³.month^{-1}, respectively (Figure 11a, Figure 11b, and Figure 11c).

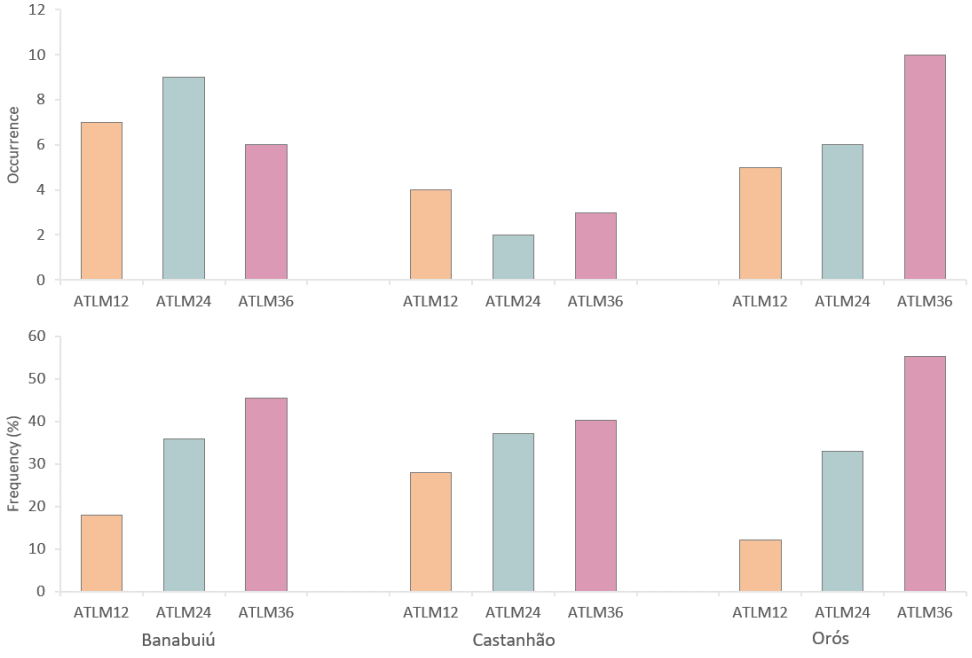

Figure 10. Number of occurrences and frequency of hydrological drought events determined by the ATLM method for the Banabuiú, Castanhão, and Orós dams, considering time factors of 12, 24, and 36 months.

By extending the time factor to 24 months, the longest-lasting hydrological drought event started in October 2014, three months earlier than the drought identified with a 12-month time factor, persisting until August 2021, totaling 84 months. This ratio remains unchanged for a time factor of 36 months, where the longest drought spanned from July 2014 to August 2020, lasting 75 months.

For time factors of 24 and 36 months, the droughts had an average duration of 17 and 32 months, respectively (Figure 11a). Their severity and average magnitude were recorded as 1,530.12 hm³ and 83.55 hm³.month^{-1} for the ATLM 24, and 5,768.36 hm³ and 149.40 hm³.month^{-1} for the ATLM 36 (Figure 11a, Figure 11b, and Figure 11c).

It is important to note that for each time factor, regardless of the reservoir, there is a specific period for analyzing hydrological drought occurrence based on the threshold level. As the time factor increases, this period decreases proportionally. This limitation was necessary to align the methodology with available reservoir monitoring data. Thus, the conclusion of the analyzed period for each time factor may not necessarily align with the termination of the last identified drought.

For the Castanhão Dam, analyzing the ATLM 12, reveals the onset of the longest and most severe drought event, spanning 52 months and peaking in severity at 17,047.61 hm³, starting in February 2016 and concluding in April 2020. Throughout this period, the reservoir's storage volume average about 5% of its total capacity, owing to the severe conditions of the

https://doi.org/10.5194/egusphere-2024-813
Preprint. Discussion started: 4 April 2024

meteorological drought that started in 2012. Consequently, besides facing significant evaporation losses, the Castanhão Dam experienced increased withdrawals to meet the demands of other watersheds that were facing water scarcity.

Regarding time factors of 24 and 36 months, the ATLM 36 exhibits a notable variation between the minimum and maximum values of duration, severity, and magnitude of the identified hydrological drought events.

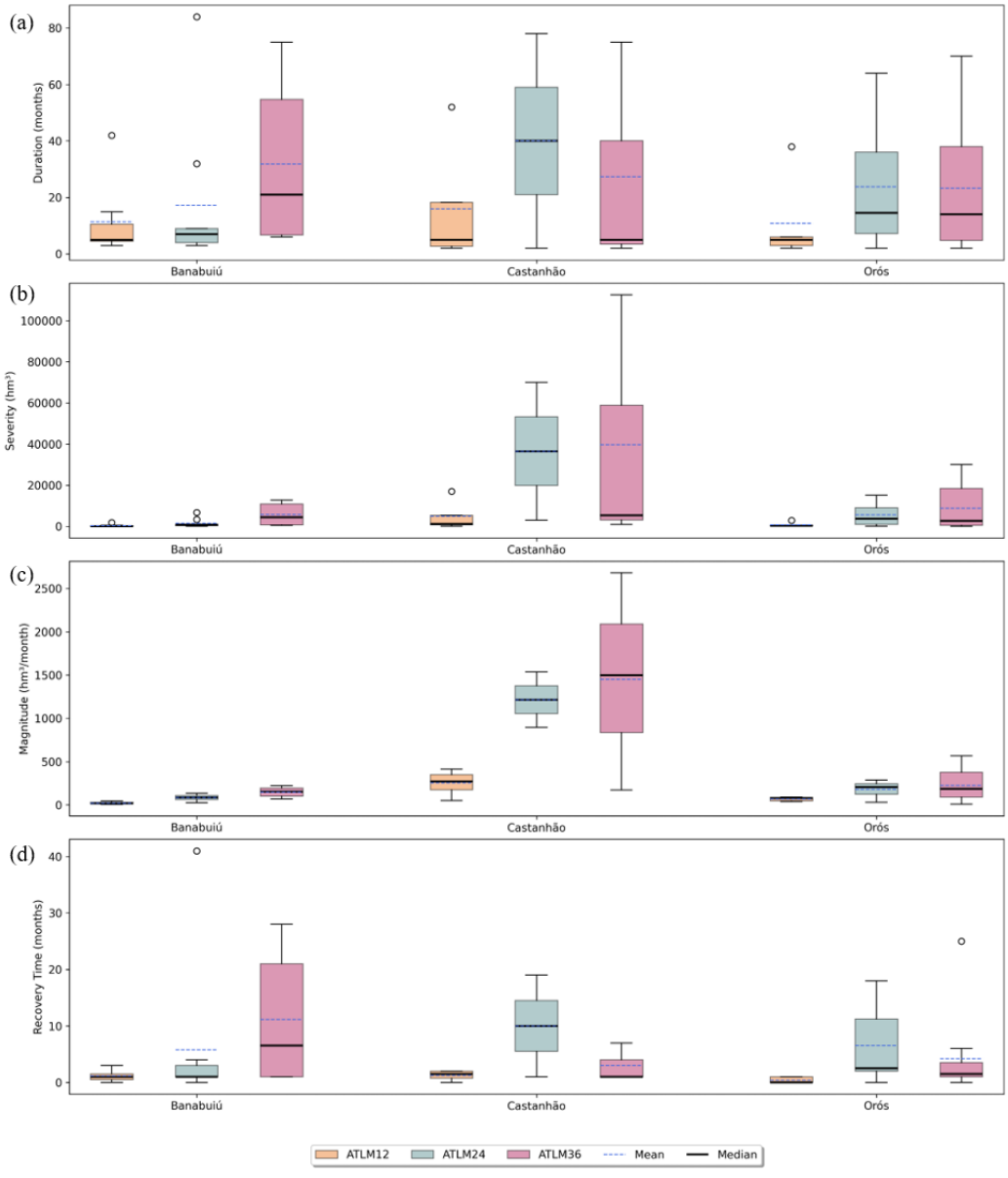

Figure 11. Characterization of hydrological drought using the ATLM for time factors with data aggregated for 12, 24, and 36 months for the Banabuiú, Castanhão, and Orós reservoirs: (a) duration (months); (b) severity (hm^3); (c) magnitude ($hm^3.month^{-1}$); (d) recovery time from drought events (months). The hollow circles represent the values of extreme events.

https://doi.org/10.5194/egusphere-2024-813
Preprint. Discussion started: 4 April 2024

For the Orós Dam, the most prolonged and severe events for the studied time factors unfolded between March 2017 and March 2020, between June 2016 and August 2021, and between December 2014 and August 2020 for ATLM 12, ATLM 24, and ATLM 36, respectively. Thus, similar to Banabuiú and Castanhão, an increase in the time factor leads to earlier onset of drought events for Orós Dam. Moreover, in the case of the Orós Dam, severity and magnitude increase as more months are aggregated to the time factor.

Oliveira et al. (2022) employed the Standardized Runoff Index (SRI) at scales with data aggregated for 3 months and 12 months to assess hydrological drought in the watershed of the Orós Reservoir, analyzing data spanning from 1982 to 2020. The SRI-12 identified a prolonged hydrological drought, commencing in the first half of 2015 and concluding in the second half of 2018. Notably, the SRI differs from the ATLM by using flow data, obtained through hydrological modeling employing MODHAC for the Upper Jaguaribe watershed.

There is observable variability in the drought recovery time among the reservoirs and the time factors used. However, in general, the peak months of hydrological drought events closely align with the final months of the events, or the peak month coincides with the month when the hydrological drought terminates. This trend is especially true noticeable for a time factor of 12 months, indicating swift recovery of reservoir volume (Figure 11d).

In the case of the Banabuiú Dam, the longest hydrological drought recovery time (41 months) occurred during the event of greatest duration and severity, according to the ATLM 24 (beginning in October 2014, peaking in April 2018, and concluding in August 2021). Similarly, for the Castanhão Dam, a similar pattern emerged, with a maximum duration of 19 months for the ATLM 24 (initiating in May 2015, reaching its peak in February 2020, and concluding in in September 2021). Finally, the Orós Reservoir exhibited the lengthiest recovery time (25 months), per the ATLM 36, for the hydrological drought event that begins in November 1992, reached its peak in February 1995, and concluded in March 1997. These results underscore the complexity dynamics of post-drought recovery and underscore the difficulty in determining the total duration of an event based solely on identifying the month of peak severity.

It is important to emphasize that the method used in this study for quantifying hydrological drought relies on the historical series of monitored stored volumes and demands of various uses within their respective watersheds, utilizing the Threshold Level Method (TLM). This approach enables the measurement of the actual water deficit, offering a more effective means of managing water resources at the local level and serving as a vital tool for operating complex water systems (Raposo et al., 2023; van Loon, 2015).

On the other hand, the use of standardized indices offers the advantage of enabling a direct and straightforward comparison of hydrological drought events across watersheds with different climates. This approach contributes to a better understanding of droughts dynamics both temporally and spatially (Quiring, 2009; Teutschbein et al., 2022). Given that the Banabuiú, Castanhão, and Orós watersheds are located in a region sharing similar climatic characteristics, the selected method proves effective for quantifying and characterizing hydrological drought, thereby serving as a valuable tool for decision-making in water resource management within these watersheds.

https://doi.org/10.5194/egusphere-2024-813
Preprint. Discussion started: 4 April 2024

3.3. Propagation from meteorological drought to hydrological drought

To ascertain which meteorological drought index (SPI or SPEI) and time scale exhibit the most pronounced or subdued response in terms of propagation time to hydrological drought, we conducted analyses encompassing combinations of SPI-12, SPI-24, SPI-36, SPEI-12, SPEI-24, and SPEI-36 with ATLM 12, 24, and 36 for the studied reservoirs. The graphic comparison is illustrated in Figure 12 to Figure 14 for Banabuiú, Figure 15 to Figure 17 for Castanhão, and Figure 18 to Figure 20 for Orós. A specific time frame was established within the series of meteorological drought indices to synchronize with the available data for hydrological drought.

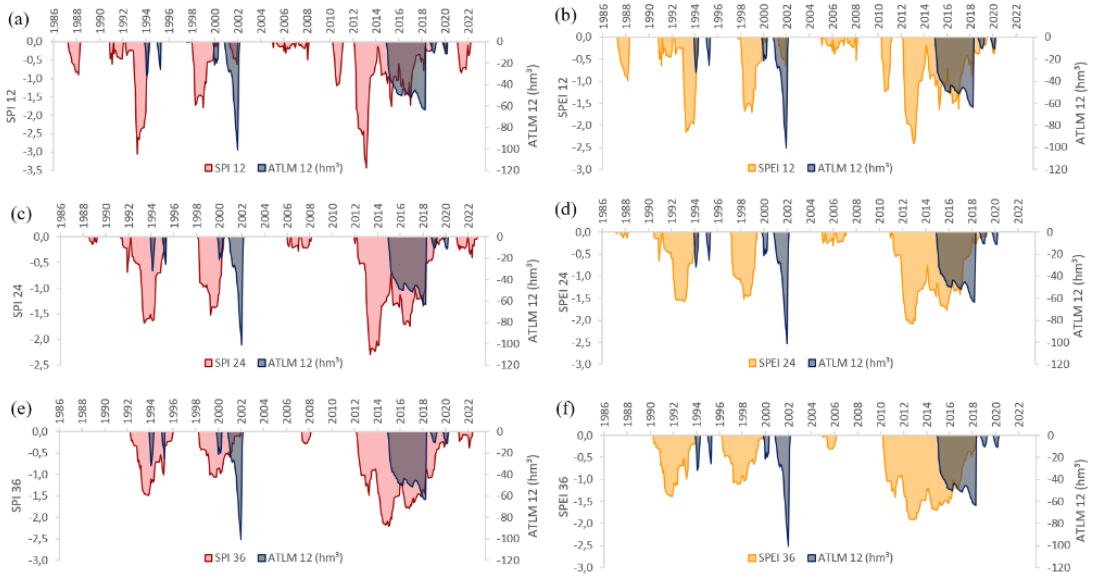

Figure 12. Propagation from meteorological drought, obtained using the SPI and SPEI indices at time scales with data aggregated for 12, 24, and 36 months, to hydrological drought, defined by the ATLM with data aggregated for 12 months, for the Banabuiú Dam.

https://doi.org/10.5194/egusphere-2024-813
Preprint. Discussion started: 4 April 2024

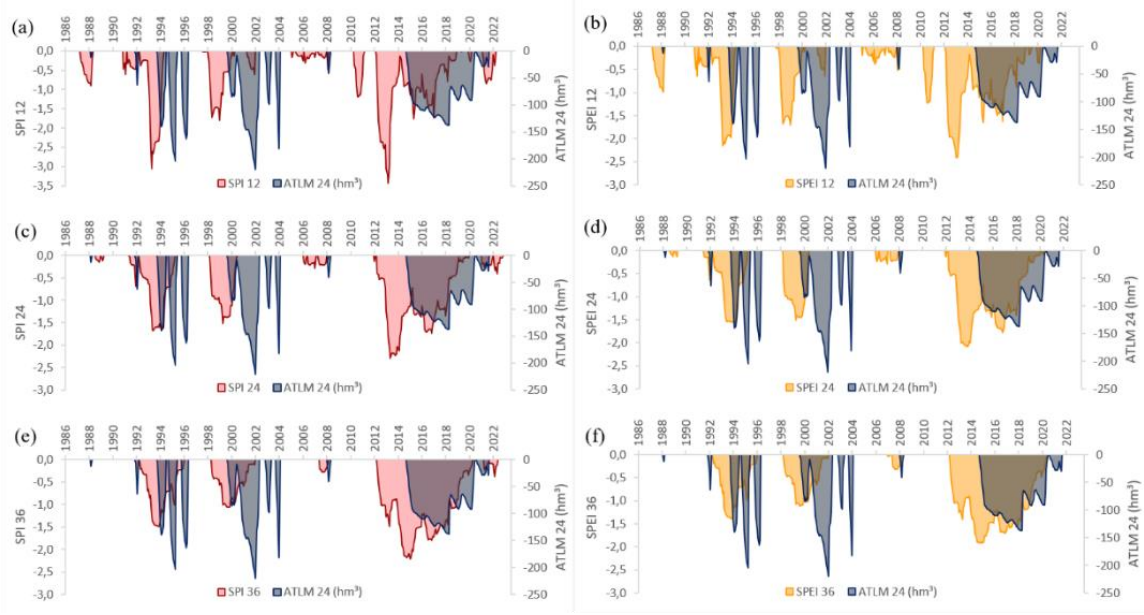

Figure 13. Propagation from meteorological drought, obtained using the SPI and SPEI indices at time scales with data aggregated for 12, 24, and 36 months, to hydrological drought, defined by the ATLM with data aggregated for 24 months, for the Banabuiú Dam.

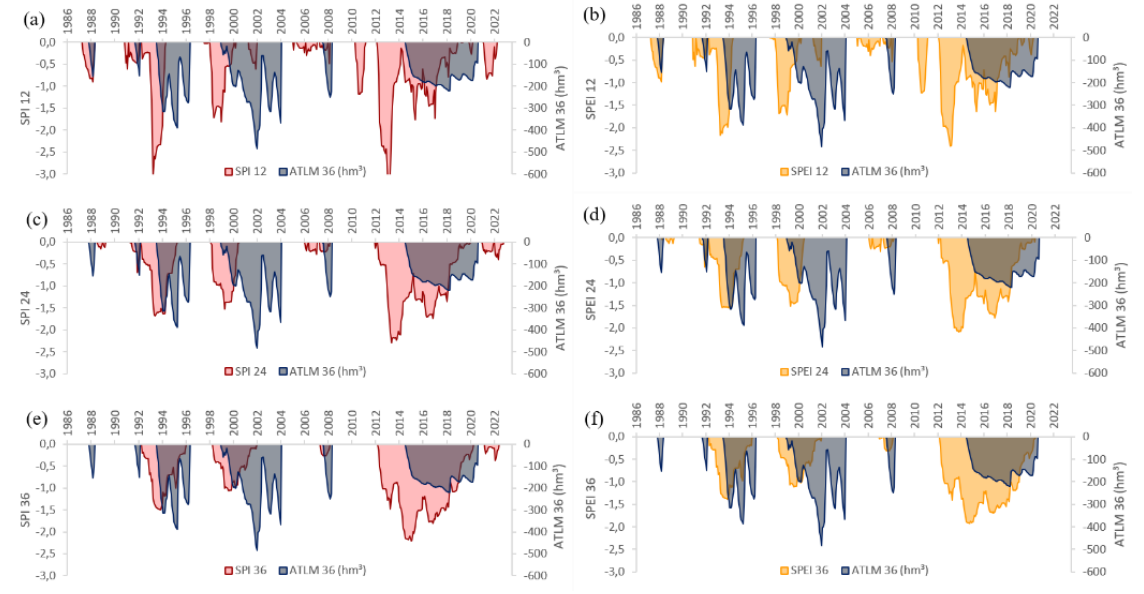

Figure 14. Propagation from meteorological drought, obtained using the SPI and SPEI indices at time scales with data aggregated for 12, 24, and 36 months, to hydrological drought, defined by the ATLM with data aggregated for 36 months, for the Banabuiú Dam.

Upon scrutinizing the drought periods identified for Banabuiú, it becomes apparent that certain events deviated from the predefined conditions. Notably, instances hydrological drought terminating before the conclusion of meteorological drought

https://doi.org/10.5194/egusphere-2024-813
Preprint. Discussion started: 4 April 2024

have been observed. This anomaly is evident in the events spanning from 2012 and 2021, particularly when using the SPI-36 and ATLM-12 indices (Figure 12e). Additionally, instances of hydrological drought occurring without preceding meteorological drought have been identified (Figure 13d, Figure 13e, Figure 13f; Figure 14d, Figure 14e, Figure 14f).

For Banabuiú, the highest prevalence of meteorological droughts transitioning to hydrological droughts was observed when utilizing the SPI and SPEI indices at a time scale with data aggregated for 12 months, coupled with ATLM with a time factor of 36 months. In this combination, the average time intervals for the onset, peak, and end of the different types of drought were 13.2, 23.2, and 16.5 months, respectively (Table 1).

Table 1. Drought propagation across the Banabuiú, Castanhão, and Orós reservoir watersheds, indicating the average time difference (in months) between the onset ($\overline{\Delta \boldsymbol{b}}$), peak ($\overline{\Delta \boldsymbol{p}}$), and conclusion ($\overline{\Delta \boldsymbol{e}}$) of meteorological and hydrological drought events. The values that have the longest propagation times are highlighted in bold.

		Banabuiú				Castanhão				Orós			
Meteor. drought	Hidrol. drought	Number of propagated droughts	$\overline{\Delta b}$	$\overline{\Delta p}$	$\overline{\Delta e}$	Number of propagated droughts	$\overline{\Delta b}$	$\overline{\Delta p}$	$\overline{\Delta e}$	Number of propagated droughts	$\overline{\Delta b}$	$\overline{\Delta p}$	$\overline{\Delta e}$
			(months)				(months)				(months)		
SPI 12	ATLM 12	3	42.7	32.3	2.3	2	13	33.5	11.5	0	-	-	-
SPEI 12		3	42.7	32.3	2.0	1	20.0	**59.0**	**18.0**	1	33.0	13	**39.0**
SPI 24		2	**68.5**	**53.5**	**2.5**	1	38.0	40.0	2.0	1	9.0	**28.0**	31.0
SPEI 24		2	67.5	47.0	**2.5**	1	38.0	40.0	2.0	3	39.0	1.3	18.0
SPI 36		1	32.0	30.0	2.0	1	**45.0**	35.0	2.0	0	-	-	-
SPEI 36		1	32.0	30.0	2.0	1	**45.0**	34.0	2.0	2	**58.0**	2.0	2.0
SPI 12	ATLM 24	4	21.3	30.8	**16.0**	1	11.0	**59.0**	**35.0**	1	25.0	**35.0**	44.0
SPEI 12		4	21.3	31.0	15.8	1	11.0	**59.0**	**35.0**	3	24.7	16.0	25.0
SPI 24		3	**29,7**	**39.0**	15.3	1	29.0	40.0	20.0	1	57.0	**35.0**	**68.0**
SPEI 24		3	29.0	34.7	15.3	1	29.0	40.0	20.0	3	26.3	7.0	16.3
SPI 36		3	29.3	33.0	8.7	1	**36.0**	35.0	19.0	3	**58.0**	34.0	44.7
SPEI 36		3	29.3	33.7	8	1	**36.0**	34.0	19.0	2	41.5	11.0	28.5
SPI 12	ATLM 36	6	13.2	23.2	16.5	2	4.5	30.5	**12.0**	4	32.8	**39.0**	47.0
SPEI 12		6	13.2	23.3	16.3	2	4.5	30.5	**12.0**	5	12.0	12.8	18.6
SPI 24		4	**16.8**	**30.5**	**17.0**	2	**21.0**	**32.5**	6.0	4	**39.3**	34.8	**50.3**
SPEI 24		4	16.3	28.5	**17.0**	2	**21.0**	**32.5**	6.0	4	12.3	10.8	18.5
SPI 36		4	13.3	23.3	9.3	2	18.5	21.5	5.0	4	39.0	28.5	40.8
SPEI 36		4	13.3	23.8	8.8	2	18.5	21.0	5.0	3	16.3	8	15.7

In the case of Castanhão, minimal drought propagation was observed across all combinations tested (Figure 15, Figure 16, and Figure 17). This outcome can be attributed to the dam's considerable water reserve capacity, which enhances its resilience to hydrological droughts. However, it is noteworthy that the prolonged meteorological drought beginning in 2012 precipitated a substantial decrease in the stored volume, ultimately plunging the reservoir into a state of hydrological drought. This propagated drought event was identified in all analyses.

https://doi.org/10.5194/egusphere-2024-813
Preprint. Discussion started: 4 April 2024

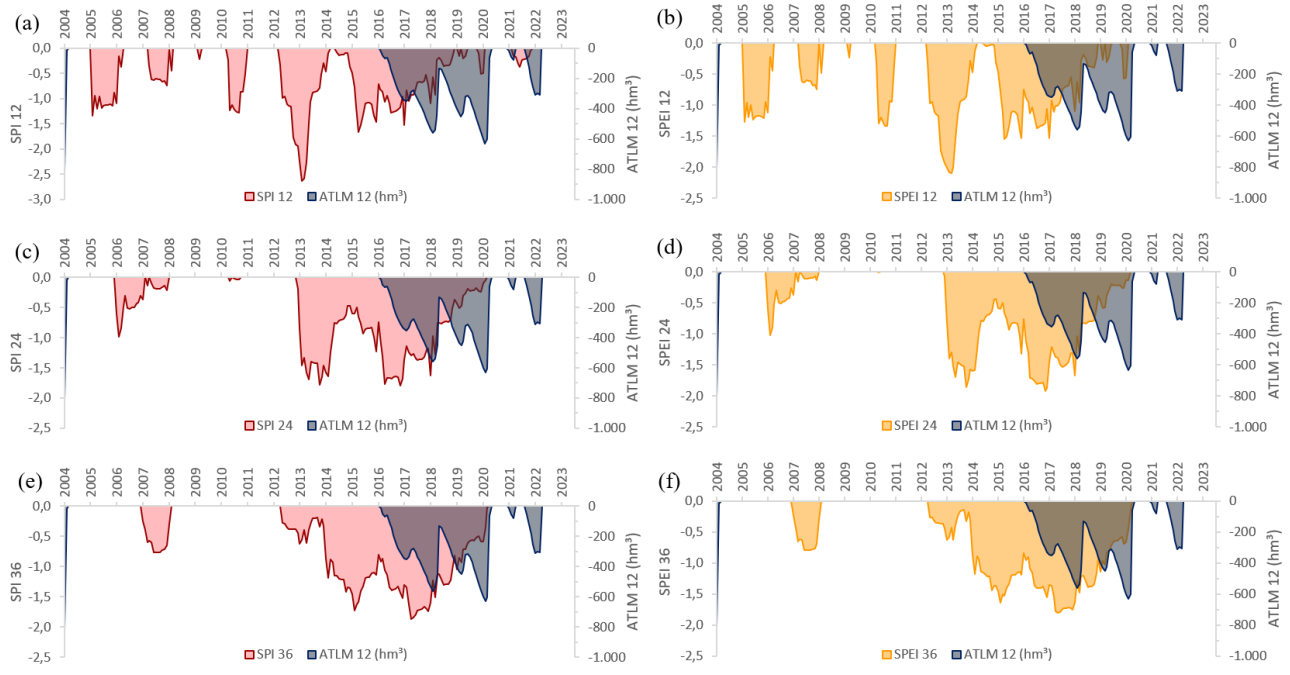

Figure 15. Propagation from meteorological drought, obtained using the SPI and SPEI indices at time scales with data aggregated for 12, 24, and 36 months, to hydrological drought, defined by the ATLM with data aggregated for 12 months, for the Castanhão Dam.

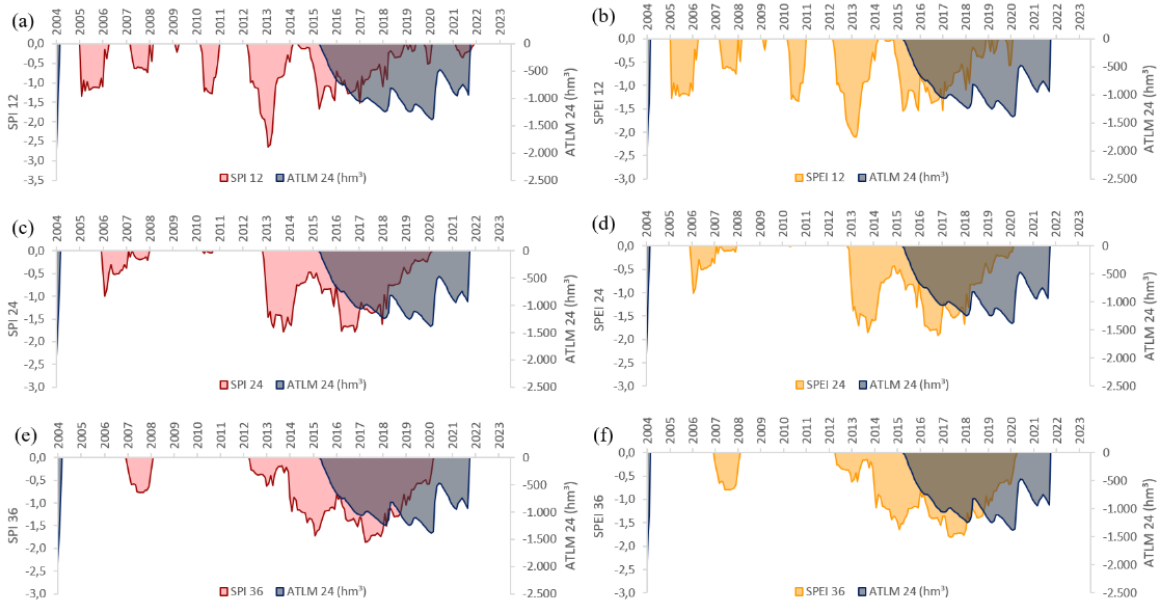

Figure 16. Propagation from meteorological drought, obtained using the SPI and SPEI indices at time scales with data aggregated for 12, 24, and 36 months, to hydrological drought, defined by the ATLM with data aggregated for 24 months, for the Castanhão Dam.

https://doi.org/10.5194/egusphere-2024-813
Preprint. Discussion started: 4 April 2024

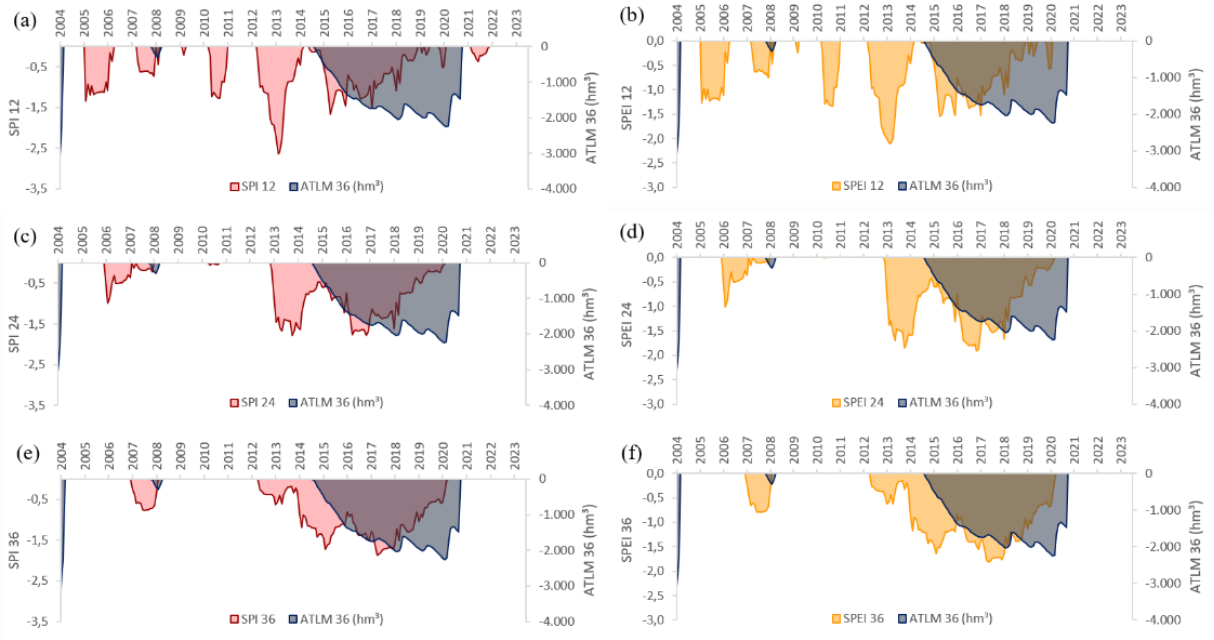

Figure 17. Propagation from meteorological drought, obtained using the SPI and SPEI indices at time scales with data aggregated for 12, 24, and 36 months, to hydrological drought, defined by the ATLM with data aggregated for 36 months, for the Castanhão Dam.

The results for Orós reveal significant variability in the number of propagated droughts among the simulated indices, indicating a more complex dynamic in drought propagation (Figure 18, Figure 19, and Figure 20). The highest number of propagated droughts was observed when using SPEI 12 and ATLM 36, with an average propagation time from the beginning of the drought of 12 months, between the peaks of 18.6 months, and between the ends of 12.8 months (Table 1).

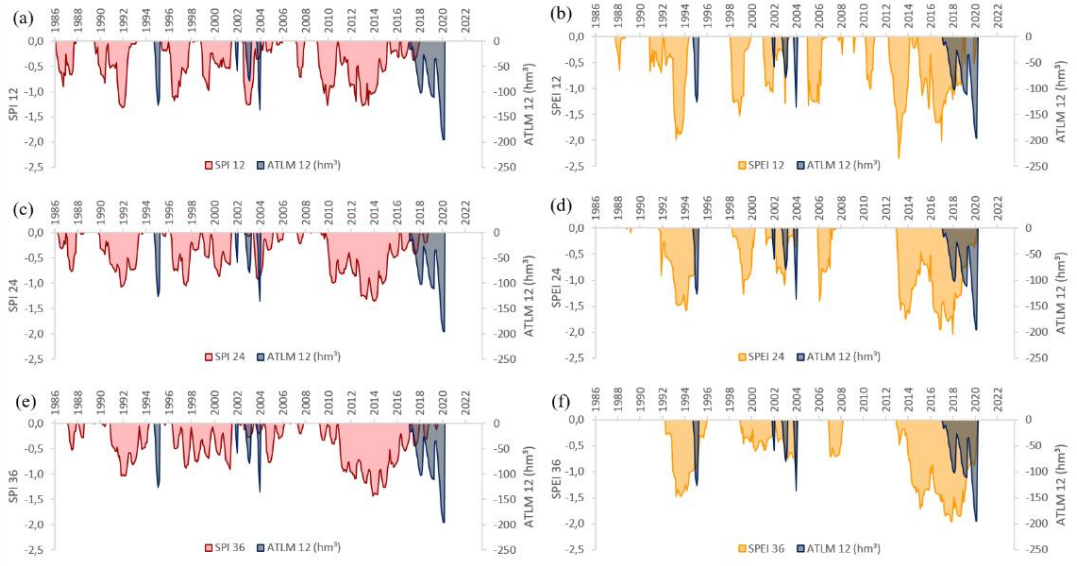

https://doi.org/10.5194/egusphere-2024-813
Preprint. Discussion started: 4 April 2024

Figure 18. Propagation from meteorological drought, obtained using the SPI and SPEI indices at time scales with data aggregated for 12, 24, and 36 months, to hydrological drought, defined by the ATLM with data aggregated for 12 months, for the Orós Dam.

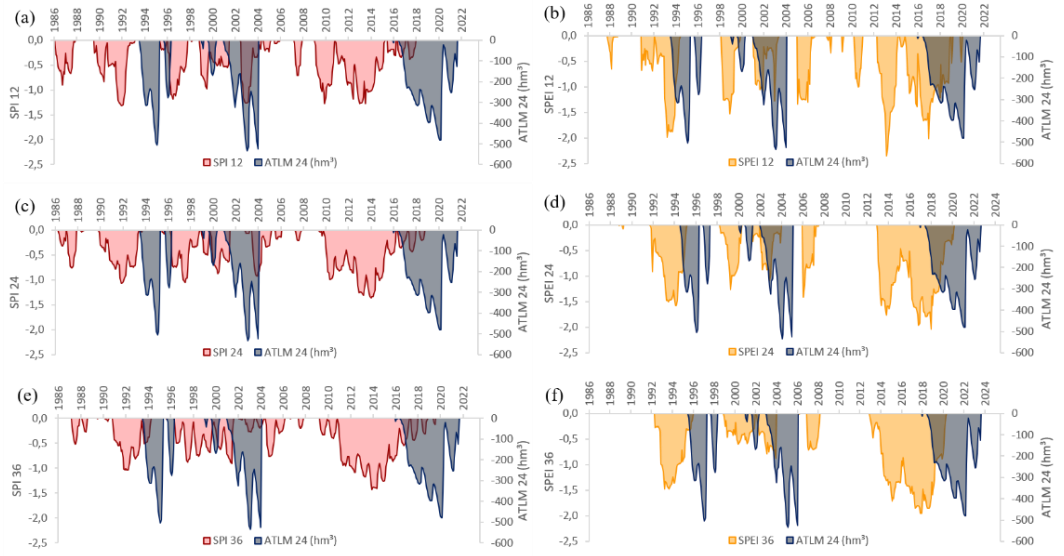

460 **Figure 19**. Propagation from meteorological drought, obtained using the SPI and SPEI indices at time scales with data aggregated for 12, 24, and 36 months, to hydrological drought, defined by the ATLM with data aggregated for 24 months, for the Orós Dam.

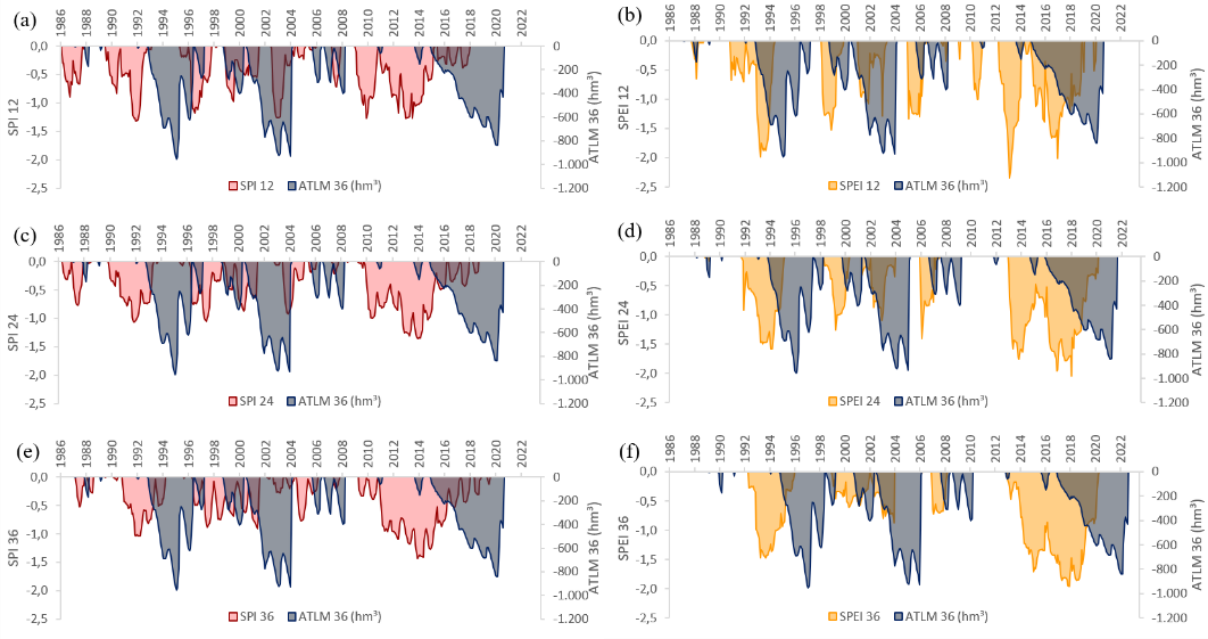

Figure 20. Propagation from meteorological drought, obtained using the SPI and SPEI indices at time scales with data aggregated for 12, 24, and 36 months, to hydrological drought, defined by the ATLM with data aggregated for 36 months, for the Orós Dam.

https://doi.org/10.5194/egusphere-2024-813
Preprint. Discussion started: 4 April 2024

Recent literature on drought propagation indicates that the transition of a meteorological drought into other drought types is often site-specific. This means that there is no standardized pattern of propagation times, even in regions with similar climates (Raposo et al., 2023).

Ideally, the propagation response between hydrological drought and meteorological drought should be linear, that is, the propagation time for each combined event of the different types of drought should be similar or equivalent (Edossa et al., 2010). However, in a given watershed, the hydrological response to the meteorological process often exhibits non-linearity due to watershed characteristics, anthropogenic activities, and climate change influences (van Loon et al., 2016; Wu et al., 2021b).

Additionally, the selection of indicators for drought identification and characterization, alongside the time scale chosen and various threshold levels, can lead to discrepancies in the propagation time results (Zhang et al., 2022b), as evidenced in our study's findings.

Regarding meteorological droughts, researchers expect that rising temperatures will significantly impact drought severity. Therefore, there is a growing advocacy for the adoption of the SPEI over SPI, as the former includes the evapotranspiration component influenced by rising temperatures (Reyniers et al., 2022; Tomasella et al., 2022; Vicente-Serrano et al., 2022). Regarding hydrological droughts, human activities such as reservoir operation, water extraction, land use changes, agricultural intensification often exert a more significant effect than climate change (Vicente-Serrano et al., 2022; Wanders and Wada, 2015). Therefore, quantifying hydrological drought stemming from such activities becomes increasingly crucial for comprehending the drought propagation process. However, generalizing the anthropogenic impact is challenging due to the complexity of human interventions in watersheds.

4 Conclusions

Meteorological drought, stemming from insufficient precipitation, can catalyze other types of droughts, underscoring the importance of comprehending variations in drought characteristics and the phenomenon of propagation to hydrological droughts from past events. This understanding is vital for devising strategies to mitigate their adverse effects.

This study utilized two meteorological drought indices, the Standardized Precipitation Index (SPI) and the Standardized Precipitation Evapotranspiration Index (SPEI), alongside with the adapted threshold level method to quantify hydrological drought. These methodologies were applied across time scales with data aggregated for 12, 24, and 36 months to identify drought periods, elucidate their characteristics, and delineate the propagation of drought in the Banabuiú, Castanhão and Orós watershed, located within the Brazilian semi-arid region.

The results indicate that, overall, there were no significant discrepancies between the SPI and SPEI indices regarding the characteristics of meteorological drought, including frequency, duration, severity, magnitude, and drought recovery, particularly in the Banabuiú and Castanhão regions. On the other hand, for the Orós watershed, the SPEI exhibited relatively higher values in drought characteristics compared to the SPI.

https://doi.org/10.5194/egusphere-2024-813
Preprint. Discussion started: 4 April 2024

The application of the adapted threshold level method for identifying hydrological drought enabling the measurement of the actual water deficit by calculating the water balance between the water in the reservoirs and the demands of various users within the watershed. This analysis was conducted across different time scales with aggregated data.

An examination of drought propagation, based on a comparison of different methods, revealed a lack of defined pattern for the onset, peak, and end intervals of the events across all tested combinations. Consequently, it is recommended to use all three methods to enable a more comprehensive analysis of drought events propagated in the watersheds.

Additionally, further research is suggested to assess drought propagation time using alternative methods that provide early warnings of hydrological drought, based on short- and long-term weather forecasts.

Code and data availability. All codes and data used in this study will be made available upon request to the corresponding author.

Author contributions. GCSM and SMOS jointly conceptualized the study. GCSM conducted collected the data, developed the methodology, and wrote the article. The results were collectively discussed and interpreted by the GCSM and SMOS. SMOS reviewed the manuscript.

Competing interests. The authors declare that they have no conflict of interest.

Acknowledgements. The authors express their gratitude to Ályson Brayner Sousa Estácio for providing recent volumetric monitoring data of the studied reservoirs. Additionally, special thanks to Mário Sérgio Freitas Ferreira Cavalcante for his contribution in creating the codes used to present the results in the article.

Financial support. The present study was conducted with the support of the Ceará Foundation for the Support of Scientific and Technological Development (FUNCAP-CE) under Normative Instruction No. 04/2019.

References

Angelidis, P., Maris, F., Kotsovinos, N., and Hrissanthou, V., 2012. Computation of Drought Index SPI with Alternative Distribution Functions. Water Resour. Manag. 26, 2453–2473. https://doi.org/10.1007/s11269-012-0026-0

Araújo Júnior, L.M., Souza Filho, F.A., Cid, D.A.C, Silva, S.M.O., and Silveira, C.S., 2020. Avaliação de índices de seca meteorológica e hidrológica em relação ao impacto de acumulação de água em reservatório: um estudo de caso para o reservatório de Jucazinho-PE. Revista AIDIS de Ingeniería y Ciencias Ambientales. 13 (2), 382-398. https://doi.org/10.22201/iingen.0718378xe.2020.13.2.65562.

Batista, C.O.N., Correia, V.M.S., and Silva, F.J.A., 2019. Hidroquímica das águas superficiais do Reservatório Banabuiú. In: Congresso Brasileiro de Engenharia Sanitária e Ambiental, 30° ed., 16 a 19 jun. 2019, Natal, Rio Grande do Norte. Anais [...]. Natal, Rio Grande do Norte.

https://doi.org/10.5194/egusphere-2024-813
Preprint. Discussion started: 4 April 2024

Bevacqua, A.G., Chaffe, P.L.B., Chagas, V.B.P., and Aghakouchak, A., 2021. Spatial and temporal patterns of propagation from meteorological to hydrological droughts in Brazil. J. Hydrol. 603, 126902. https://doi.org/10.1016/j.jhydrol.2021.126902.

Chen, N., Li, R., Zhang, X., Yang, C., Wang, X., Zeng, L., Tang, S., Wang, W., Li, D., and Niyogi, D., 2020. Drought propagation in northern China plain: a comparative analysis of GLDAS and MERRA-2 datasets. J. Hydrol. 588, 125026. https://doi.org/10.1016/j.jhydrol.2020.125026.

Chen, Y.D., Zhang, Q., Xiao, M., and Singh, V.P., 2013. Evaluation of risk of hydrological drought by the trivariate Plackett copula in the East River basin (China). Nat Hazards. 68, 529–547. https://doi.org/10.1007/s11069-013-0628-8

Choat, B., Brodribb, T.J., Brodersen, C.R., Duursma, R.A., López, R., and Medlyn, B.E., 2018. Triggers of tree mortality under drought. Nature. 558, 531–539. https://doi.org/10.1038/s41586-018-0240-x.

Companhia de Gestão dos Recursos Hídricos (COGERH), 2023. Seminário de Alocação Negociada das Águas dos Vales Jaguaribe e Banabuiú. Açudes Banabuiú, Castanhão e Orós. Ceará, 06 de julho de 2023.

De Brito, Y.M.A., De Brito, H.C., Rufino, L.A., and Braga, C.F.C., 2021. Panorama da seca plurianual 2012-2018 no semiárido brasileiro: Impactos hidrológicos, agrícolas e medidas de convivência. Des. e Meio Ambiente, 58, 12-26. http://dx.doi.org/10.5380/dma.v58i0.74667

Ding, Y., Gong, X., Xing, Z., Cai, H., Zhou, Z., Zhang, D., Sun, P., and Shi, H., 2021. Attribution of meteorological, hydrological and agricultural drought propagation in different climatic regions of China. Agric. Water Manag. 255, 106996. https://doi.org/10.1016/j.agwat.2021.106996.

Edossa, D.C., Babel, M.S., and Das, G., 2010. Drought analysis in the Awash river basin, Ethiopia. Water Resour. Manag. 24 (7), 1441–1460. https://doi.org/10.1007/s11269-009-9508-0

Eltahir, E., and Yeh, J.F., 1999. On the asymmetric response of aquifer water level to floods and droughts in Illinois. Water Resour. Res. 35 (4), 1199–1217. https://doi.org/10.1029/1998WR900071.

Fleig, A.K., Tallaksen, L.M., Hisdal, H., and Demuth, S., 2006. A global evaluation of streamflow drought characteristics. Hydrol. Earth Sys. Sci., Copernicus Publications, 10, p. 535–552. https://doi.org/10.5194/hess-10-535-2006

Gonçalves, S.T.N., Vasconcelos Júnior, F.C., Silveira, C.S., Costa, J.M.F., and Marcos Junior, A.D., 2023. Avaliação de Índices de Seca no Monitoramento Hidrológico de Reservatórios Estratégicos do Ceará, Brasil. Revista Brasileira de Meteorologia, 38, e38230018. http://dx.doi.org/10.1590/0102-77863810018

Gumus, V., 2023. Evaluating the effect of the SPI and SPEI methods on drought monitoring over Turkey. J. Hydrol. 626, 130386. https://doi.org/10.1016/j.jhydrol.2023.130386.

Guo, Y., Huang, S., Huang, Q., Leng, G., Fang, W., Wang, L., and Wang, H., 2020. Propagation thresholds of meteorological drought for triggering hydrological drought at various levels. Sci. Total Environ. 712, 136502. https://doi.org/10.1016/j.scitotenv.2020.136502.

Ho, S., Tian, L.u., Disse, M., Tuo, and Y.e., 2021. A new approach to quantify propagation time from meteorological to hydrological drought. J. Hydrol. 603, 127056. https://doi.org/10.1016/j.jhydrol.2021.127056.

https://doi.org/10.5194/egusphere-2024-813
Preprint. Discussion started: 4 April 2024

Huang, S., Chang, J., Leng, G., and Huang, Q., 2015. Integrated index for drought assessment based on variable fuzzy set theory: a case study in the Yellow River basin, China. J. Hydrol. 527, 608–618. https://doi.org/10.1016/j.jhydrol.2015.05.032.

Keyantash, J., National Center for Atmospheric Research Staff (Eds)., 2023. Last modified 2023-08-19. "The Climate Data Guide: Standardized Precipitation Index (SPI) [online]." Available from https://climatedataguide.ucar.edu/climate-data/standardized-precipitation-index-spi. Accessed on 20 January 2024.

Li, L., She, D., Zheng, H., Lin, P., and Yang, Z.L., 2020. Elucidating Diverse Drought Characteristics from Two Meteorological Drought Indices (SPI and SPEI) in China. J. Hydrometeorol. 21, 1513–1530. https://doi.org/10.1175/jhm-d-19-0290.1.

Ma, F., Luo, L., Ye, A., and Duan, Q., 2019. Drought characteristics and propagation in the semiarid Heihe River basin in Northwestern China. J. Hydrometeorol. 20, 59–77. https://doi.org/10.1175/JHM-D-18-0129.1.

Marengo, J.A., Alves, L.M., Alvala, R.C.S., Cunha, A.P., Brito, S., and Moraes, O.L.L., 2018. Climatic characteristics of the 2010-2016 drought in the semiarid Northeast Brazil region. Annals of the Brazilian Academy of Sciences. 90 (2 Suppl. 1), 1973–1985. https://doi.org/10.1590/0001-3765201720170206.

Marengo, J.A., Cunha, A.P., and Alves, L.M., 2016. A seca de 2012-15 no semiárido do Nordeste do Brasil no contexto histórico. Climanálise. 3 (1), 49-54.

Mckee, T.B., Doesken, N.J., and Kleist, J., 1993. The Relationship of Drought Frequency and Duration to Time Scales, Paper Presented at 8th Conference on Applied Climatology. American Meteorological Society, Anaheim, CA.

Medeiros, G.C.S., Maia, A.G., and Medeiros, J.D.F., 2019. Assessment of two different methods in predicting hydrological drought from the perspective of water demand. Water Resour. Manag. 33, 1851–1865. https://doi.org/10.1007/s11269-019-02218-7.

Mishra, A.K., and Singh, V.P., 2010. A review of drought concepts. J. Hydrol. 391 (1–2), 202–216. https://doi.org/10.1016/j.jhydrol.2010.07.012.

Mohor, G.S., and Mendiondo, E.M., 2017. Economic indicators of hydrologic drought insurance under water demand and climate change scenarios in a Brazilian context. Ecol. Econ. 140, 66–78. https://doi.org/10.1016/j.ecolecon.2017.04.014.

Oliveira, T.A., Souza Filho, F.A., and Pontes Filho. J.D.A., 2022. Relações entre secas meteorológicas, agrícolas e hidrológicas em uma região semiárida do estado do Ceará. In: Secas e Cheias: Modelagem e Adaptação aos extremos hidrológicos no contexto da variabilidade e mudança do clima. Org.: Souza Filho, F.A., Reis Júnior, D.S., Galvão, C.O. Fortaleza, CE. Ed. Expressão Gráfica. 1260p.

Pandey, R.P., Mishra, S.K., Singh, R., and Ramasastri, K.S., 2008. Streamflow Drought Severity Analysis of Betwa River System (India). Water Resour. Manage. 22, 1127–1141. https://doi.org/10.1007/s11269-007-9216-6

Pei, Z., Fang, S., Wang, L., and Yang, W., 2020. Comparative Analysis of Drought Indicated by the SPI and SPEI at Various Timescales in Inner Mongolia. China. Water. 12. https://doi.org/10.3390/w12071925.

https://doi.org/10.5194/egusphere-2024-813
Preprint. Discussion started: 4 April 2024

Pontes Filho, J.D., Souza Filho, F.A., Martins, E.S.P.R., and Studart, T.M.C., 2020. Copula-based multivariate frequency analysis of the 2012-2018 Drought in Northeast Brazil. Water. 12 (3), 834. https://doi.org/10.3390/w12030834

Quiring, S.M., 2009. Monitoring drought: an evaluation of meteorological drought indices. Geogr. Compass. 3, 64–88. https://doi.org/10.1111/j.1749-8198.2008.00207.x.

Rabelo, U.P., and Lima Neto, I.E., 2018. Efeito de secas prolongadas nos recursos hídricos de uma região semiárida: uma análise comparativa para o Ceará. DAE, 66 (212), 61-79. http://dx.doi.org/10.4322/dae.2018.023.

Raposo, V.M.B., Costa, V.A.F., and Rodrigues, A.F., 2023. A review of recent developments on drought characterization, propagation, and influential factors, Sci. Total Environ. 898, 165550. https://doi.org/10.1016/j.scitotenv.2023.165550.

Reyniers, N., Osborn, T.J., Addor, N., and Darch, G., 2022. Projected changes in droughts and extreme droughts in Great Britain strongly influenced by the choice of drought index. Hydrol. Earth Sys. Sci. 27 (5), 1151–1171. https://doi.org/10.5194/hess-2022-94.

SRH, 2011. Inventário Ambiental dos Açudes Castanhão, Orós e Banabuiú. Secretaria dos Recursos Hídricos do Estado do Ceará, 379p.

Sung, J.H., and Chung, E.S., 2014. Development of streamflow drought severity-duration-frequency curves using the threshold level method. Hydrol. Earth Syst. Sci. 18, 3341–3351. https://doi.org/10.5194/hess-18-3341-2014

Tallaksen, L.M., Madsen, H., and Clausen, B., 1997. On the definition and modelling of streamflow drought duration and deficit volume. Hydrol. Sci. J. 42, 15–33. https://doi.org/10.1080/02626669709492003

Teutschbein, C., Quesada Montano, B., Todorovic, A., and Grabs, T., 2022. Streamflow droughts in Sweden: spatiotemporal patterns emerging from six decades of observations. J. Hydrol. Reg. Stud. 42. https://doi.org/10.1016/j.ejrh.2022.101171.

Tomasella, J., Cunha, A.P.M.A., Simões, P.A., and Zeri, M., 2022. Assessment of trends, variability and impacts of droughts across Brazil over the period 1980–2019. Nat. Hazards. 116 (2), 2173–2190. https://doi.org/10.1007/S11069-022-05759-0.

van Huijgevoort, M.H.J., Hazenberg, P., van Lanen, H.A.J., and Uijlenhoet, R., 2012. A generic method for hydrological drought identification across different climate regions. Hydrol. Earth Syst. Sci. 16, 2437–2451. https://doi.org/10.5194/hess-16-2437-2012.

van Loon, A.F., 2015. Hydrological drought explained. WIREs Water. 2, 359–392. https://doi.org/10.1002/wat2.1085.

van Loon, A.F., Gleeson, T., Clark, J., Van Dijk, A.I.J.M., Stahl, K., Hannaford, J., Di Baldassarre, G., Teuling, A.J., Tallaksen, L.M., Uijlenhoet, R., Hannah. D.M., Sheffield, J., Svoboda, M., Verbeiren, B., Wagener, T., Rangecroft, S., Wanders, N., and Van Lanen, H.A.J., 2016. Drought in the anthropocene. Nature Geosci., 9 (2): 89–91. https://doi.org/10.1038/ngeo2646.

van Loon, A.F., and Laaha, G., 2015. Hydrological drought severity explained by climate and catchment characteristics. J. Hydrol. 526, 3–14. https://doi.org/10.1016/j.jhydrol.2014.10.059.

https://doi.org/10.5194/egusphere-2024-813
Preprint. Discussion started: 4 April 2024

Vicente-Serrano, S.M., Beguería, S., and López-Moreno, J.I., 2010. A Multiscalar Drought Index Sensitive to Global Warming: The Standardized Precipitation Evapotranspiration Index. J. Clim. 23, 1696–1718. https://doi.org/10.1175/2009JCLI2909.1.

Vicente-Serrano, S.M., Peña-Angulo, D., Beguería, S., Domínguez-Castro, F., Tomás- Burguera, M., Noguera, I., Gimeno-Sotelo, L., and el Kenawy, A., 2022. Global drought trends and future projections. Philos. Trans. A Math. Phys. Eng. Sci. 380 (2238) https://doi.org/10.1098/rsta.2021.0285.

Wanders, N., and Wada, Y., 2015. Human and climate impacts on the 21st century hydrological drought. J. Hydrol. 208-220. https://doi.org/10.1016/j.jhydrol.2014.10.047.

Wang, M., Jiang, S., Ren, L., Xu, C., Yuan, F. Liu, Y., and Yang, X., 2020. An approach for identification and quantification of hydrological drought termination characteristics of natural and human-influenced series. J. Hydrol. 590, 125384. https://doi.org/10.1016/j.jhydrol.2020.125384.

Wilhite, D.A., and Glantz, M.H., 1985. Understanding: the Drought Phenomenon: The Role of Definitions. Water Int. 10 (3), 111–120. https://doi.org/10.1080/02508068508686328.

Wilhite, D.A., and Pulwarty, R.S., 2018. Drought and Water Crises, edited by: Wilhite, D. and Pulwarty, R.S., CRC Press, Second edition. | Boca Raton: CRC Press. 1st ed. published in 2005. https://doi.org/10.1201/b22009.

WMO, 2012. 1900: Standardized Precipitation Index User Guide. Geneva, 2012.

Wu, J., Chen, X., Yao, H., Gao, L., Chen, Y., and Liu, M., 2017. Non-linear relationship of hydrological drought responding to meteorological drought and impact of a large reservoir. J. Hydrol. 551, 495–507. https://doi.org/10.1016/j.jhydrol.2017.06.029.

Wu, J., and Chen, X., 2019. Spatiotemporal trends of dryness/wetness duration and severity: The respective contribution of precipitation and temperature. Atmos. Res. 216, 176–185. https://doi.org/10.1016/j.atmosres.2018.10.005.

Wu, J., Yuan, X., Yao, H., Chen, X., and Wang, G., 2021a. Reservoirs regulate the relationship between hydrological drought recovery water and drought characteristics. J. Hydrol. 603, 127127.

Wu, J., Chen, X., Yao, H., and Zhang, D., 2021b. Multi-timescale assessment of propagation thresholds from meteorological to hydrological drought. Sci. Total Environ. 765, 144232 https://doi.org/10.1016/J.SCITOTENV.2020.144232.

Xing, Z., Ma, M., Zhang, X., Leng, G., Su, Z., Lv, J., Yu, Z., and Yi, P., 2021. Altered drought propagation under the influence of reservoir regulation. J. Hydrol. 603, 127049. https://doi.org/10.1016/j.jhydrol.2021.127049.

Xu, Y., Zhang, X., Wang, X., Hao, Z., Singh, V.P., and Hao, F., 2019. Propagation from meteorological drought to hydrological drought under the impact of human activities: A case study in northern China. J. Hydrol. 579, 124147. https://doi.org/10.1016/j.jhydrol.2019.124147.

Yevjevich, V., 1967. An objective approach to definitions and investigations of continental hydrologic droughts. Hydrology Papers, 23, Colorado State University, Fort Collins, USA. https://doi.org/10.1016/0022-1694(69)90110-3

Zelenhasic, E., and Salvai, A., 1987. A Method Of Streamflow Drought Analysis. Water Resour. Res. 23 (1), 156 – 168. https://doi.org/10.1029/WR023i001p00156

https://doi.org/10.5194/egusphere-2024-813
Preprint. Discussion started: 4 April 2024

Zhang, L., Jiao, W., Zhang, H., Huang, C., and Tong, Q., 2017. Studying drought phenomena in the Continental United States in 2011 and 2012 using various drought indices. Remote Sens. Environ. 190, 96-106. https://doi.org/10.1016/j.rse.2016.12.010

Zhang, T., Su, X., Zhang, G., Wu, H., Wang, G., and Chu, J., 2022a. Evaluation of the impacts of human activities on propagation from meteorological drought to hydrological drought in the Weihe River Basin, China, Sci. Total Environ. 819, 153030. https://doi.org/10.1016/j.scitotenv.2022.153030.

Zhang, X., Hao, Z., Singh, V.P., Zhang, Y., Feng, S., Xu, Y., and Hao, F., 2022b. Drought propagation under global warming: characteristics, approaches, processes, and controlling factors. Sci. Total Environ. 838, 156021. https://doi.org/10.1016/j.scitotenv.2022.156021.

Zhou, Z., Shi, H., Fu, Q., Ding, Y., Li, T., Wang, Y., and Liu, S., 2021. Characteristics of Propagation From Meteorological Drought to Hydrological Drought in the Pearl River Basin. J. Geophys. Res. Atmos. 126 (4). https://doi.org/10.1029/2020JD033959.